NEUROSCIENCE
RESEARCH ARTICLE
C. Castillo et al. / Neuroscience 376 (2018) 204–223

Extracellular Application of CRMP2 Increases Cytoplasmic Calcium through NMDA Receptors

Cecilia Castillo,[a]* Juan Carlos Martinez,[a] Marines Longart,[a] Lisbeth García,[a] Marianela Hernández,[a] Jeismar Carballo,[a] Héctor Rojas,[b] Lorena Matteo,[a] Liliana Casique,[c] José Leonardo Escalona,[c] Yuryanni Rodríguez,[a] Jessica Rodriguez,[a] Deyanell Hernández,[a] Domingo Balbi[a] and Raimundo Villegas[a]

[a] *Unidad de Neurociencias, Instituto de Estudios Avanzados IDEA, Caracas 1080, Venezuela*

[b] *Instituto de Inmunología, Facultad de Medicina, Universidad Central de Venezuela, Caracas 1051, Venezuela*

[c] *Depto. de Biología Celular, Universidad Simón Bolívar, Caracas 1080, Venezuela*

Abstract—Collapsin Response Mediator Protein 2 (CRMP2) is an intracellular protein involved in axon and dendrite growth and specification. In this study, CRMP2 was identified in a conditioned media derived from degenerated sciatic nerves (CM). On cultured rat hippocampal neurons, acute extracellular application of CM or partially purified recombinant CRMP2 produced an increase in cytoplasmic calcium. The increase in cytoplasmic calcium was mostly mediated through NMDA receptors, with a minor contribution of N-type VDCC, and it was maintained as long as CM was present. By using live-labeling of CRMP2, Ca^{2+} channel binding domain 3 (CBD3) peptide derived from CRMP2, and recombinant CRMP2, we demonstrated that that this effect was mediated by an action on the extracellular side of the NMDA receptor. This is the first report of an extracellular action of CRMP2. Prolonged exposure to extracellular CRMP2, may contribute to neuronal calcium dysregulation and neuronal damage.

Key words: excitotoxicity, CBD3 peptide, calcium imaging, calcium dysregulation confocal, hippocampal neurons.

INTRODUCTION

Collapsin Response Mediator Proteins (CRMP) are cytosolic phosphoproteins that regulate many neuronal functions. So far, five CRMP isoforms (CRMP1–5) have been identified in vertebrates (Schmidt and Strittmatter, 2007). Each CRMP isoform has a specific function. CRMP2 plays a role in neuronal polarity (Yoshimura et al., 2005) by interacting with many proteins that modulate microtubule dynamics (Suzuki et al., 2003) promoting axon elongation (Inagaki et al., 2001). Intracellular actions of CRMP2 also comprises the regulation of surface expression of N-methyl-D-aspartate receptor (NMDAr) (Al-Hallaq et al., 2007; Brittain et al., 2011b; Brustovetsky et al., 2014; François-Moutal et al., 2015) and modulation of N-type voltage-dependent calcium channels (VDCCs) surface trafficking (Brittain et al., 2009; Chi et al., 2009; Wang et al., 2010). Moreover, CRMP2 has been implicated in several neurological pathologies (Khanna et al., 2012) such as neuropathic pain (François-Moutal et al., 2015; Moutal et al., 2016, 2017a,b,c,d,e; Xie et al., 2016), Alzheimer (Yoshida et al., 1998), Parkinson (Kuter et al., 2016), multiple sclerosis (Petratos et al., 2012) and traumatic injuries, such as sciatic nerve crush (Suzuki et al., 2003).

Our group has been studying a conditioned medium derived from *in vitro* degenerated sciatic nerves (CM) that induces neuritogenic activity in PC12 cells (Villegas et al., 1995). Chronic exposure to CM also resulted in an increase of N- and P/Q Ca^{2+} currents (Castillo et al., 2001) and of a large conductance calcium-activated K^+ currents (K_{Ca}) (Castillo et al., 2006) in PC12 cells. Ca^{2+} is the principal signaling molecule in mammalian neurons as in other cells (Berridge, 1998; Grienberger and Konnerth, 2012) and it is essential for normal function; however, its dysregulation can lead to cell death. Extracellular Ca^{2+} influx is mediated by ionotropic glutamate receptors (IGr), nicotinic acetylcholine

*Correspondence to: C. Castillo, Unidad de Neurociencias, Instituto de Estudios Avanzados, IDEA, Carretera Nacional Hoyo de la Puerta–Baruta, Valle de Sartenejas, Baruta, Estado Miranda 1080, Venezuela.
E-mail address: cjcastillo.w@gmail.com (C. Castillo).

Abbreviations: $[Ca^{2+}]_i$, intracellular calcium concentration; AP-5, (2R)-amino-5-phosphonovaleric acid; CBD3, calcium channel binding domain 3; CM, conditioned media; CNQX, 6-cyano-7-nitroquinoxaline-2,3-dione; CRMP2, Collapsin Response Mediator Protein 2; FBS, fetal bovine serum; HA-966, (±) 3-amino-1-hydroxy-pyrrolidin-2-one; HEPES, 4-(2-hydroxyethyl)-1-piperazineethanesulfonicacid; Igr, ionotropic glutamate receptors; K_{Ca}, large conductance calcium-activated K^+ currents; NGS, normal goat serum; NMDA, N-methyl-D-aspartate; NMDAr, N-methyl-D-aspartate receptor; OpCM, optic CM; PBS, phosphate-buffered saline; PC12 cells, cell line derived from a rat pheochromocytoma of the adrenal medulla; PFA, paraformaldehyde; Schw-CM, Schwann cell CM; VDCC, voltage-dependent calcium channel.

https://doi.org/10.1016/j.neuroscience.2018.02.002
0306-4522/

receptors, voltage-dependent Ca^{2+} channels (VDCCs), and transient receptor potential type C channels (Grienberger and Konnerth, 2012). An important IGr is the NMDAr, which is involved in many neuronal functions (Cline et al., 1987; Kleinschmidt et al., 1987). NMDAr dysfunction has also been associated with many neurological disorders including pain (Davies and Lodge, 1987; Dickenson and Sullivan, 1987). Excessive NMDAr activity leads to excessive increase in intracellular calcium ($[Ca^{2+}]_i$) that leads to excitotoxicity and neuronal death (Moutal et al., 2015).

The goal of this study was to identify which molecule within the CM was responsible for the CM-mediated increase in Ca^{2+} currents and investigate its molecular mechanism. It was found that the CM contained CRMP2 (CRMP2-CM) and it was demonstrated that acute application of CRMP2-CM evoked intracellular Ca^{2+} increase ($[Ca^{2+}]_i$) in rat hippocampal cultures. As stated above, intracellular CRMP2 has been shown to modulate NMDAr and N-type VDCC, hence here, it was explored whether extracellular CRMP2 could also affect $[Ca^{2+}]_i$ by acting on one or both of these channels. It was found that, in hippocampal neurons, extracellular application of CRMP2-CM evoked an increase in $[Ca^{2+}]_i$ by acting on NMDAr and to a minor extent on N-type VDCCs, and demonstrated that these effects were mediated by extracellular interactions. Additionally, molecular modeling suggested that the C-terminal domain of CRMP2 might bind to extracellular regions of the NMDAr. This is the first demonstration that CRMP2 may act extracellularly to activate NMDAr and by doing so produce an increase in $[Ca^{2+}]_i$.

EXPERIMENTAL PROCEDURES

Animals

Sprague–Dawley adult male rats (*Rattus novergicus*) were used to extract sciatic and optic nerves to prepare conditioned media (CM). Hippocampal cell cultures were prepared using 19-day-old rat embryos from pregnant rats (*Rattus novergicus*) and postnatal (P0–P2) rat newborns (either sex). Animals were kept and sacrificed following the regulations of the Instituto de Estudios Avanzados, in accordance with the National Institutes of Health Guide for the Care and Use of Laboratory Animals (NIH Publications No. 80–23), revised in 1996. Care was taken to use the minimal amount of animals and all precautions were taken to minimize animal suffering

Reagents

Rabbit polyclonal Anti-CRMP-2 antibody for Western Blots and immunofluorescence (ab62661) and for immunodepletion (ab129082) were from Abcam (Cambridge, MA). Other reagents were obtained from different sources: Tat-CBD3 peptide (BioTrends, Cologne, Germany); ω-conotoxin GVIA (Alomone Labs, Jerusalem, Israel); AP-5 and MK-801 (Tocris, Bioscience, Minneapolis, MN); NMDA, CNQX and nifedipine (Sigma, St. Louis, MI) and CBD3 peptide (Biomatik, Cambridge, Ontario, Canada).

CM preparation

CM was prepared as previously described (Villegas et al., 1995), with some modifications. Briefly, eight sciatic nerves from Sprague–Dawley adult male rats were extracted and cultured in 6 ml serum-free DMEM (Dulbecco Modified Eagle's Medium) for 7 days in an incubator (5% CO_2, 37 °C). At day 8, the nerves were transferred to new flasks containing fresh serum-free DMEM. CM was collected every 24 h from day 9 until day 11, and stored at −70 °C. To standardize the amount of calcium in the CMs, pools of 9–11 days CM were dialyzed against a Ca^{2+} and Mg^{2+}-free-HEPES buffer (in mM, 123 NaCl, 5 KCl, 5 $NaHCO_3$, 10 HEPES, and 10 mM glucose pH 7.4) using a 3500 MW cutoff membrane at 4 °C (Spectra-Por; dialysis membranes, Spectrum laboratories, Rancho Dominguez, CA). Three buffer changes were made until phenol red from DMEM became visually undetectable, (about ≈18 h). CM was aliquoted and stored at −70 °C. CMs were supplemented with 2 mM $CaCl_2$ before the calcium imaging experiments as required.

Optic CM (OpCM) preparation

Groups of 12 pairs of optic nerves were obtained from adult male rats (same rats used to prepare sciatic CM) were cultured in 6-mL serum-free DMEM sera for 12 days. OpCM were collected either after 1–4 days or 9–11 days of culture. The medium was changed every 4 days by fresh DMEM, and stored at −70 °C until use. OpCM was dialyzed in the same way as sciatic CM.

Schwann Cell CM (Schw-CM) Schw-CM was prepared as described before (Villegas et al., 2005) and dialyzed as indicated above.

Hippocampal neuronal cultures

Hippocampal neuronal cultures were prepared from 19-day-old rat embryos as previously described (Brewer, 1995) and used after 6–9 days in *in vitro* culture. Embryonic hippocampal cells were cultured in Neurobasal medium (Gibco-Invitrogen, Waltham, MA), supplemented with 2% B27 (Gibco-Invitrogen), 0.5 mM Glutamax (Gibco-Invitrogen), penicillin (100 U/ml), streptomycin (100 μg/ml) and maintained in an incubator (5% CO_2 at 37 °C). Alternatively, cultures from P0–P2 rat newborns (either sex) were prepared as previously described (Nunez, 2008). Briefly, cells were dissociated and seeded in Neurobasal A medium supplemented with 10% FBS, 0.5 mM Glutamax, penicillin (100 U/ml), and streptomycin (100 μg/ml). Cells were kept and cultured in Neurobasal A medium supplemented with 2% B27, 0.5 mM Glutamax, penicillin (100 U/ml), streptomycin (100 μg/ml) and maintained in an atmosphere of 5% CO_2 at 37 °C. Hippocampal cells were seeded on 15 mm diameter coverslips, pre-coated with 0.1 mg/mL poly-D-lysine (Sigma, St. Louis, MI) for 1 h at 37 °C and rinsed three times with MilliQ water.

Calcium imaging

Cells were loaded with the fluorescent Ca^{2+} indicator Fura-2 AM (5 μM) (Molecular Probes, Eugene, OR) for 60 min at 37 °C and cytoplasmic Ca^{2+} ($[Ca^{2+}]_i$) changes were measured at 30 °C as previously described (Corrales et al., 2003; Sutachan et al., 2006; Castillo et al., 2011). Coverslips were mounted on an open perfusion chamber (type RC-25F; Warner Instruments, Hamden, CT). Cells were perfused (250 μL/min) with a Mg^{2+}-free-HEPES buffer [(in mM) 140 NaCl, 5 KCl, 5 $NaHCO_3$, 10 HEPES, 2 $CaCl_2$ and 10 glucose, pH 7.35] for 30 min prior to any stimulation. All drugs, NMDA (100 μM), MK-801 (50 μM), AP-5 (100 μM), CNQX (200 μM) and nifedipine (5 μM), were prepared in the Mg^{2+}-free-HEPES buffer and added directly on top of the cells by using the Octaflow focal perfusion system (ALA Scientific, Farmingdale, NY). The solution containing NMDA (100 μM) also contained Glycine (10 μM) unless otherwise indicated. Measurements were done using an IonOptix imaging system (Ion Optix Co., Milton, MA). The excitation wavelengths for Fura-2 (340 nm and 380 nm) were alternately generated (0.9 s) by passing a transmitted light source thorough separate filters (340 nm and 380 nm filters, Chroma Technology Corp. Bellows Falls, Vermont) with a Hyperswitch light source system (IonOptix Corporation). The emitted fluorescence from individual cells was filtered with a fluorescence barrier filter (510 nm, Chroma Technology Corp.) and collected with a CCD camera (Myocam Camera-IonOptix Co.). The relative changes in $[Ca^{2+}]_i$ are given by the ratio of the emission of Fura-2 at the barrier filter generated by the alternate excitation at 340 nm and 380 nm (ratio (340/380)). Either at the beginning or at the end of the experiment cells were depolarized with a pulse of K^+ (100 mM) to check that the recorded neurons were healthy as determined by their capacity to display a depolarization-evoked increase in $[Ca^{2+}]_i$. K^+ pulses applied before the CM did not affect the reproducibility of CM-evoked $[Ca^{2+}]_i$ increases. In some experiments, an ATP pulse (100 μM) was applied to distinguish neurons from glial cells, since only glias respond to ATP with an increase in $[Ca^{2+}]_i$ (Castillo et al., 2013). Cells were selected individually, each neuron was considered as an individual data, and each experiment included the cells from a given coverslip.

Experiments were first done with 10 μM tat-CBD3 alone, but this concentration increased basal calcium and most of the cells were not able to regulate calcium levels to basal levels (data not shown), therefore, we used 5 μM. When tat-CBD3 (5 μM) was perfused, at times a small transient increase was observed, hence agonists were applied after the basal $[Ca^{2+}]_i$ level was reached following tat-CBD3 application.

During calcium imaging experiments the substances (agonists or antagonists) that were applied focally (e.g., 2 s application) were prepared using the specific perfusion media (e.g., without or with CM) being use in the experiment, unless otherwise indicated.

Quantification of glutamate and glycine by HPLC

Quantification of glutamate and glycine was performed by HPLC as already described (Chiku et al., 2009), with some modifications. Briefly, lyophilized samples (1 mL) were resuspended in 100 μL of MiliQ H_2O and diluted 1:1 with trichloroacetic acid (50%). Samples were centrifuged (12,000×*g*) for 10 min at room temperature and 10 μL of the supernatants were diluted 1:5 with 0.2 M borate buffer pH 9.6, filtered through 0.22-μm membranes and derivatized with 10 μL of o-phthalaldehyde solution (15 mM o-phthaldialdehyde, 30 mM 2-mercaptoethanol, and 10% methanol in 0.2 M sodium borate buffer, pH 9.6). After incubation for 1 min at room temperature, a portion of the mixture (20 μL) was injected into an Atlantis® dC18 5 μm, 4.6 × 25 0 mm column (Waters, Millford, MA). Amino acids were eluted at a flow rate of 1 mL/min with buffers A (80% 0.1 M sodium acetate, 20% methanol, pH 4.75) and B (20% 0.1 M sodium acetate, 80% methanol, pH 4.75) using the gradient described by (Chiku et al., 2009). The HPLC system consisted of a 1525 binary pump and 2475 multi λ fluorescence detector (Waters, Millford, MA), set at 340-nm excitation and 450-nm emission wavelengths.

Preparation of samples for peptide sequence analysis

Samples were prepared from band excised in the range of 58–60 kDa as described before (Malavé et al., 2003). These samples were sequenced (microsequencing) at Harvard Microchemistry Facility, Harvard University (Cambridge, MA).

CRMP2 identification in the CM

Aliquots of 2–6 μg of sciatic or optic CM were analyzed by SDS–PAGE, using 10% acrylamide gels, and electrotransferred to nitrocellulose membranes using a trans-blot semi-dry system (Bio-Rad, Hercules, CA) for 1 h. After blotting, membranes were blocked (5% non-fat dry milk, 0.1% Tween-20 in Tris-buffered saline 50 mM Tris pH 8, 150 mM NaCl) for 2 h, and incubated with the CRMP-2 antibody diluted 1:2000 overnight at 4 °C. Finally, blots were incubated with the goat anti-rabbit HRP-conjugated secondary antibody diluted 1:10,000 (ImmunoPure Goat Anti-Rabbit IgG, Peroxidase Conjugated, Thermo Scientific). Immunoreactive species were identified with Pierce ECL-Western Blotting Substrate (Pierce, Thermo Fisher Scientific) or Chemiluminescent Peroxidase Substrate-1 (Sigma–Aldrich) and imaged using the ChemiDoc XRS+ imaging system with an Image Lab program, version 5.2.1 (Bio-Rad Laboratories, Inc, Hercules, California). The estimated concentration of CRMP2 in the CM is ~170 nM.

Removal of CRMP2 protein from CM (IP-CRMP2-CM)

Protein A-Sepharose (Prot-A) (GE Healthcare, Buckinghamshire, UK) was pre-hydrated with PBS at least for 24 h before use. CRMP2 antibody (ab129082,

Abcam, Cambridge, MA) (dilution 1:50) was bound to Prot-A by incubation for 1 h at room temperature. Aliquots of dialyzed CM were pre-absorbed with Prot-A for 1 h at room temperature with constant agitation (45 rpm; Mylab Rotamix SRLM1, Seoulin Bioscience Co. Seoul, Korea). The mixture was spun at 350×*g* for 4 min. The pre-absorbed MC was added to the Prot-A, with and without bound CRMP2, and incubated overnight at 4 °C with constant agitation (45 rpm; Mylab Rotamix SRLM1). The following day the mixture was centrifuged at 325×*g* for 4 min and the supernatant was used immediately for imaging experiments the same day.

Live labeling of exogenous CRMP2 in hippocampal cells

Hippocampal cells were extracted from newborn rat brains (P0–P2) and cultured for 6 to 10 days (DIV 6–10), as indicated before. The day of the experiment cells were incubated with CM or Neurobasal medium (NB), in the presence of the CRMP2 antibody (1:1000) and Wheat Germ Agglutinin-Alexa Fluor 488-Conjugated (WGA-Alexa 488, 1:500; W1126, Thermo Fisher Scientific; Waltham, MA), a membrane surface marker, at 28 °C during 30 min. After that, cells were fixed with 4% PFA during 20 min at room temperature, blocked with 10% normal goat serum (NGS), followed by incubation with the goat anti-rabbit-Alexa 594 secondary antibody diluted in 2% NGS (1:400, A11037, Thermo Fisher Scientific) and DAPI (1:10,000, cat #268298, Calbiochem, Darmstadt, Germany), and mounted in fluorescent protecting media (Mowiol-Dabco) (Dabco cat# D2522, Sigma, Saint Louis, MO; Mowiol 4-88 Reagent, Calbiochem-EMD Biosciences, La Jolla, CA). Additionally, to visualize neurons and their neurites, some cells were incubated with NB, fixed as above, permeabilized (0.25% triton X-100, 10 min at room temperature) and then labeled with CRMP2 and MAP2 antibodies, another cells were incubated with CM and CRMP2 antibody, fixed and permeabilized as above and they were incubated with MAP-2 antibody (1:5000, Sigma–Aldrich cat# M44013). Then, all cells were incubated with goat anti-rabbit-Alexa 594 and goat anti-mouse-Alexa 488 secondary antibodies, as indicated above. Cells were visualized with a Confocal Laser Scanning Biological Microscope (FLUOVIEW FV1000 Olympus America Inc.) using an UplanFLN 40×/1.30 oil lens and 405, 473 and 559 nm lasers. Images were taken on three color channels (green, red and blue) using the FV-10ASW version 02.01.01.04 software (Olympus America Inc.). Image processing and co-localization analysis were performed with the Fiji Image J software (NIH, Bethesda, MD).

Expression and purification of recombinant CRMP2

A plasmid (pET28b–CRMP2) containing the coding sequence for the mouse CRMP2 gene, fused to a 6×HIS tag peptide at the N-terminus, was kindly supplied by Dr. Rajesh Khanna (Department of Pharmacology, University of Arizona). CRMP2 was produced in 1 L of LB medium using the *E. coli* Rosetta (DE3)pLysS bacterial strain (EMD Millipore, Billerica, MA) and the protein was partially purified from the bacterial supernatant by affinity chromatography using a nickel-Sepharose column (HiTrap IMAC FF, GE Healthcare, Piscataway, NJ). Partially purified CRMP2 was dialyzed against water and Mg^{2+}-free-HEPES buffer, quantified and used for calcium imaging. The concentration range used for rCRMP2 was between 30 nM and 300 nM. For perfusion experiments with rCRMP2 ~150 nM was used.

In silico docking of CRMP2

To assess the possibility that CRMP2 could bind to the NMDAr on the extracellular side, we used CABSdock software (http://biocomp.chem.uw.edu.pl/CABSdock). The extracellular N-terminal side of the GluN2B chain from the NMDAr (PDB No. 4pe5) was chosen for docking with the CBD3 peptide, which represents de C-terminal side of CRMP2.

Analysis and statistics

The areas of the CM and NMDA-evoked transient increases in cytoplasmic calcium ($[Ca^{2+}]_i$) were measured by taking as baseline the value observed prior to the NMDA-evoked $[Ca^{2+}]_i$ response and using the Clampfit 10 software (Molecular Devices, Sunnyvale CA). In experiments where pulses were applied, values were normalized to the first CM pulse. n = total number of individual neurons pooled from different imaging experiments (N). Most of the imaging experiments are from different neuronal preparations. Values are reported as median ± interquartile range (IQR). Each set of data was evaluated using D'Agostino & Pearson omnibus normality test to verify if values come from a Gaussian distribution. Most of the data sets did not pass this test, so non-parametric statistics were used. Comparisons with more than two groups were evaluated through non-parametric Kruskal–Wallis followed by Dunn's multiple comparison post-test with corrected p values for multiple comparisons. Comparisons of two groups were done using Wilcoxon signed rank test or Mann–Whitney test. All data were analyzed using the GraphPad Prism 6.0 software (GraphPad Software, San Diego CA). Data are plotted as box and whiskers, boxes represent 25th-75th percentiles, the median is the horizontal line and whisker show the range of the data. Two-tailed statistical tests were used and a significance level = 0.05.

RESULTS

CRMP2 is present in a fraction of CM

CM was fractionated using several chromatographic techniques to help identify molecules responsible for the neuritogenic activity on PC12 cells (Villegas et al., 2000). Neuritogenic activity was detected in the fraction with a molecular mass range from 50 to 70 kDa when separated on SDS–PAGE gels (Villegas et al., 2000; Malavé et al., 2003). These protein bands were isolated and

prepared for peptide analyses, as previously described (Malavé et al., 2003).

Three partial peptide sequences that matched exclusively with the dihydropyrimidase related protein-2 (Collapsin Response Mediator Protein-2, CRMP2) (Fig. 1A) were found by microsequencing. Using an anti-CRMP2 antibody, a 58–60-kDa band was detected in the CM. Similarly, CRMP2 was detected in brain (~63 kDa), hippocampal lysates (bands ranging from 63–70 kDa) and in CM from optic nerves (OpCM, ~63 kDa). Two bands of ~ 68–70 kDa were detected in CM obtained from cultivated Schwann cells (SchwCM). These results indicate that CRMP2 is likely released from the cells/nerves to the culture medium of the

A

```
NP001099187.1 (DPYSL-2) MSYQGKKNIPRITSDRLLIKGGKIVNDDQSFYADIYMEDGLIKQIGENLIVPGGVKTIEA   60
AAK64497.1    (CRMP-4)  MSYQGKKNIPRITSDRLLIKGGRIVNDDQSFYADIYMEDGLIKQIGDNLIVPGGVKTIEA   60
NP037066.1    (DPYSL-3) MSYQGKKNIPRITSDRLLIKGGRIVNDDQSFYADIYMEDGLIKQIGDNLIVPGGVKTIEA   60
NP037065.1    (DPYSL-4) MSFQGKKSIPRITSDRLLIKGGKIVNDDQSFHADLYVEDGLIKQIGENLIVPGGIKTIDA   60
NP037064.1    (CRMP-1)  MSHQGKKSIPHITSDRLLIRGGRIINDDQSFYADVYLEDGLIKQIGENLIVPGGVKTIEA   60
AAB03280.1    (rCRMP-1) MSHQGKKSIPHITSDRLLIRGGRIINDDQSFYADVYLEDGLIKQIGENLIVPGGVKTIEA   60
AAB07042.1    (CRMP)    MSYQGKKSIPHITSDRLLIRGGRIINDDQSFYADVYLEDGLIKQIGENLIVPGGVKTIEA   60
                        **.****.**:********:**:*:******:**:*:********:*******:***:*

NP001099187.1 (DPYSL-2) HSRMVIPGGIDVHTRFQMPDQGMTSADDFFQGTKAALAGGTTMIIDHVVPEPGTSLLAAF   120
AAK64497.1    (CRMP-4)  NGKMVMPGGIDVHTHFQMPYKGMTTVDDFFQGTKAALAGGTTMIIDHVVPEPESSLTEAY   120
NP037066.1    (DPYSL-3) NGKMVMPGGIDVHTHFQMPYKGMTTVDDFFQGTKAALAGGTTMIIDHVVPEPESSLTEAY   120
NP037065.1    (DPYSL-4) HGLMVLPGGVDVHTRLQMPVLGMTPADDFCQGTKAALAGGTTMILDHVFPDAGVSLLAAY   120
NP037064.1    (CRMP-1)  NGRMVIPGGIDVNTYLQKPSQGMTSADDFFQGTRAALAGGTTMIIDHVVPEPGSSLLTSF   120
AAB03280.1    (rCRMP-1) NGRMVIPGGIDVNTYLQKPSQGMTSADDFFQGTRAALAGGTTMIIDHVVPEPGSSLLTSF   120
AAB07042.1    (CRMP)    NGRMVIPGGIDVNTYLQKPSQGMTSADDFFQGTRAALAGGTTMIIDHVVPEPGSSLLTSF   120
                        :. **:***:**:* :* *  *** .*** ***:**********:***.*:   **  ::

                                        < . . . >

NP001099187.1 (DPYSL-2) SAKTHNSALEYNIFEGMECRGSPLVVISQGKIVLEDGTLHVTEGSGRYIPRKPFPDFVYK   480
AAK64497.1    (CRMP-4)  SAKNHQSVAEYNIFEGMELRGAPLVVICQGKIMLEDGNLHVTQGAGRFIPCSPFSDYVYK   480
NP037066.1    (DPYSL-3) SAKNHQSVAEYNIFEGMELRGAPLVVICQGKIMLEDGNLHVTQGAGRFIPCSPFSDYVYK   480
NP037065.1    (DPYSL-4) SAKSHNLNVEYNIFEGVECRGMPTVVISQGRVVLEDGNLLVTPGAGRFIPRKTFPDFVYK   480
NP037064.1    (CRMP-1)  TAKSHKSTVEYNIFEGMECHGSPLVVISQGKIVFEDGNISVSKGMGRFIPRKPFPEHLYQ   480
AAB03280.1    (rCRMP-1) TAKSHKSTVEYNIFEGMECHGSPLVVISQGKIVFEDGNISVSKGMGRFIPRKPFPEHLYQ   480
AAB07042.1    (CRMP)    TAKSHKSTVEYNIFEGMECHGSPLVVISQGKIVFEDGNISVSKGMGRFIPRKPFPEHLYQ   480
                        :**.*:   *******:* :* * ***.**::::***.: *: * **:** . * :.:*:

                                        < . . . >
```

B

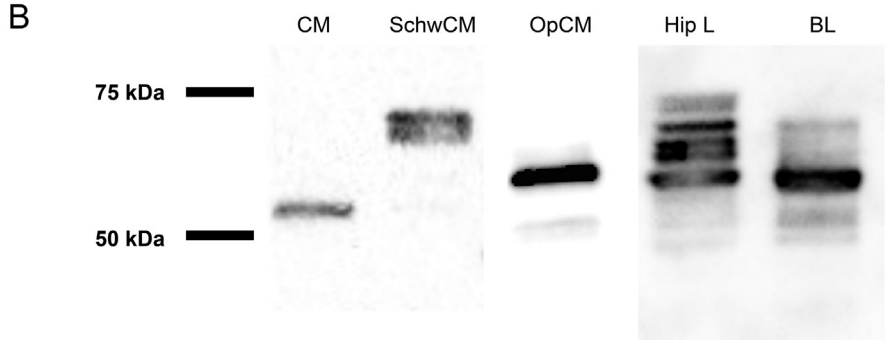

Fig. 1. CRMP2 is present in the CM. (A) Amino acid alignment of the four CRMP isoforms belonging to the genus *Rattus norvegicus*. Figure shows the amino acid sequences found in the GenBank for the CRMP proteins and the sequences of the three peptides (bold, underlined) obtained by microsequencing a 58–60 kDa SDS–PAGE gel band from CM. All three peptides only matched with a 100% identity to the CRMP2 (DPYRL-2) protein. GenBank accession numbers are indicated at the left of the alignment. Amino acid numbers are indicated on the right of the alignment. < . . . >: parts of the alignment omitted. Key denoting conserved sequence (*), conservative mutations (:), semi-conservative mutations (.), and non-conservative mutations (). Alignment was done with the Clustal Omega program (http://www.ebi.ac.uk/Tools/msa/clustalo). (B) A Western Blot showing the bands recognized by the CRMP2 antibody in different lysates: hippocampus (10 μg HipL); whole brain (10 μg BL); Schwann cell CM (6 μg, Schw CM); Sciatic nerve CM (6 μg, CM); and optic nerve CM (2 μg OpCM). Relative molecular weights (Std) are indicated in kDa. Each WB was repeated at least 3 times.

various CMs (Fig. 1B). Similar molecular weights for CRMP2 found in sciatic and optic CMs, have been reported previously (Goshima et al., 1995). Both isoforms have also been detected in the peripheral nerve side of DRGs and the molecular weight found in sciatic CM is similar to that reported for peri-CRMP2. The latter, is a C-terminal truncated form of CRMP2 (Katano et al., 2006). During brain development, it has been reported a 58-kDa isoform. This isoform when transfected into cultured cortical neurons suppressed axonal growth (Rogemond et al., 2008).

Stimulation of hippocampal neurons with CM induces $[Ca^{2+}]_i$ increase and this effect is counteracted by immunodepletion of CRMP2 from the CM

Having identified CRMP2 in the CM (CRMP2-CM), it was tested whether or not this protein affected intracellular Ca^{2+} regulation when applied extracellularly. Previously, it was shown that in PC12 cells, chronic exposure to CM resulted in the increase of a large conductance Ca^{2+}-activated K^+ currents (K_{Ca}) (Castillo et al., 2006). This CM effect was only detected when intracellular Ca^{2+} was elevated (Castillo et al., 2006). Therefore, here it was investigated if acute-extracellular application of CM could enhance the intracellular Ca^{2+} concentration ($[Ca^{2+}]_i$) in hippocampal neuronal cultures.

Hippocampal neurons loaded with Fura-2 AM responded to short pulses (2 s) of CM with an increase in $[Ca^{2+}]_i$ (Fig. 2A). Consecutive pulses applied every 5 min resulted in responses (areas under the curves) that decreased between 12 to 23% after the first pulse (Fig. 2B). Normalized areas to the first CM pulse showed that decreases among consecutive pulses were significant, indicating that there was a significant but low level of desensitization. When CM was perfused for several minutes (Fig. 2C), a sustained $[Ca^{2+}]_i$ increase was maintained as long as CM was present ($n = 294$ neurons; $N = 22$ experiments); however, a continual decrease in the magnitude of the response was observed with consecutive CM exposures. If CM was maintained longer than 12 min, 84% of the cells (19 neurons, $N = 2$ experiments) were not able to regulate their intracellular Ca^{2+} levels once CM was removed, and the focal application of NMDA or KCl pulses after the long CM exposure resulted in no response or a small response indicative that cells were no longer healthy (Fig. 2 H-I). Additionally, we studied the effect of different dilutions of the CM (Fig. 2D-E) and showed that the effect was concentration dependent. A 10-fold dilution of the CM still evoked a strong response that yielded a peak that was13.5% smaller than that evoked by the undiluted CM (median = 13.5%, IQR = −0.04–29, $n = 50$ cells, $N = 3$ experiments), hence this dilution was used for some of the experiments described below.

It was investigated if the CM-evoked increase in $[Ca^{2+}]_i$ required the presence of extracellular Ca^{2+}. The response to a CM pulse was highly decreased when extracellular Ca^{2+} was reduced by using a bath solution containing 0 Ca^{2+} and 0.5 mM EGTA (Fig. 2F). The quantification (Fig. 2G) showed that the peak values (median) in 0 Ca^{2+} decreased to 0.13 (IQR = 0.08 – 0.2) and the area values decreased to 0.29 (IQR = 0.2 – 0.4). These experiments confirmed the requirement of extracellular Ca^{2+} for the CM-evoked increase in intracellular Ca^{2+}.

Given the presence of CRMP2 in the CM, it was investigated whether CRMP2-CM was implicated in the CM-evoked increase in $[Ca^{2+}]_i$. This was performed by immunodepleting CRMP2 from the CM using an anti-CRMP2 antibody. The CM-evoked $[Ca^{2+}]_i$ was decreased by 60% when CRMP2 was immunodepleted (IQR = 28 – 71; $p < 0.0001$; while the response to CM pre-absorbed with Protein A was comparable to that of control CM (Fig. 3A-B). Fig. 3C shows a western blot of the CM preabsorbed with protein A and the CRMP2-immunodepleted CM. The densitometric analysis revealed that about 20% of CRMP2 remained in the CM following immunoprecipitation which may contribute to the observed residual $[Ca^{2+}]_i$ increase observed when using CRMP2-immunodepleted CM. These results indicate that CRMP2 in the CM contributes to the observed CM-evoked increase in cytoplasmic Ca^{2+}.

OpCM and SchwCM have similar effect than sciatic CM

To investigate whether or not the CM effect was restricted to sciatic nerve CM, the effect of CM from other sources was studied. First, it was analyzed the effect of CM derived from optical nerves (OpCM) that are from the central nervous system and found that OpCM also evoked a $[Ca^{2+}]_i$ increase in hippocampal neurons (Fig. 4A). Similarly, CM obtained from Schwann cells (SchwCM) evoked a $[Ca^{2+}]_i$ increase in hippocampal neurons (Fig. 4C). The $[Ca^{2+}]_i$ increases evoked by OpCM and SchwCM were comparable to that evoked by sciatic CM (Fig. 4B and 4D). These results suggest that CRMP2 may be released from both peripheral and central injured nerves. Moreover, the results with SchwCM suggested that CRMP2 may also be secreted by non-injured cells. Hence, extracellular CRMP2 may play a role in normal and in nerve injury states. It was also found that CM-evoked an increase in $[Ca^{2+}]_i$ in cortical and DRG neurons (data not shown). These results suggest that CRMP2-evoked $[Ca^{2+}]_i$ increase may be a conserved mechanism that contribute to the regulation of intracellular Ca^{2+} in various neuronal tissues, under normal and injured conditions.

CM induces the $[Ca^{2+}]_i$ increase via NMDAr activation

To identify the mechanism mediating the CM-evoked increase in $[Ca^{2+}]_i$, we tested the effect of antagonists to various extracellular Ca^{2+} influx mediators, like VDCC and ionotropic glutamate receptors (NMDAr, AMPA and kainate receptors) (Grienberger and Konnerth, 2012). Given the strong and wide role of NMDArs in neuronal communication, the effect of a non-competitive irreversible NMDAr antagonist, MK-801 was tested. First CM was perfused until a plateau response was reached and then, CM supplemented with MK-801 (50 μM) was perfused (Fig. 5A). MK-801 decreased the

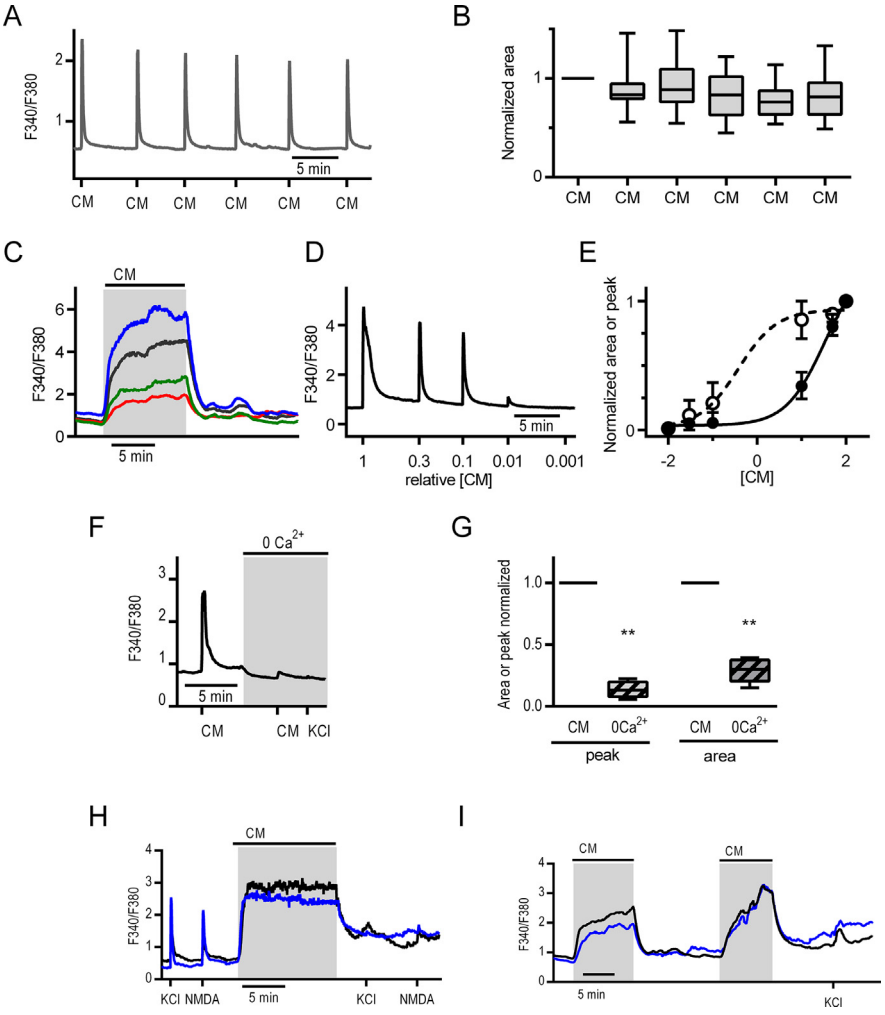

Fig. 2. CM induces $[Ca^{2+}]_i$ increases in hippocampal neurons. (A) Example of a Fura-2 ratio trace showing the $[Ca^{2+}]_i$ increases evoked by consecutive CM pulses. Two second pulses were applied with 5 min intervals. (B) Box and whiskers plot showing the normalized CM-evoked median responses (area of the transient $[Ca^{2+}]_i$ increase). Normalized areas to the first CM pulse showed that differences between pulses were significant ($p = 0.002$, $p = 0.0101$, $p = 0.0013$ for the first pulse vs second, third and fourth pulse respectively, $p = 0.0064$ for the sixth pulse, and $p < 0.0001$ for the fifth pulse; first, second and third pulse $n = 31$, fourth $n = 25$, fifth $n = 21$ and sixth $n = 13$ cells, 4 experiments; Kruskal–Wallis test: $H = 28.94$, df = 5, with Dunn's post hoc test). (C) Examples of Fura-2 ratio traces of the evoked $[Ca^{2+}]_i$ increase when the CM is applied for several minutes. $[Ca^{2+}]_i$ remains elevated as long as the CM is present, each trace corresponds to the response of a different neuron. (D) Effect of the dilution of CM on the evoked $[Ca^{2+}]_i$ increase. Representative trace of the response to different CM dilutions. (E) Summary of medians ± IQR of normalized areas (filled circles) and peaks (open circles) of the CM dilution effect on the $[Ca^{2+}]_i$ increase. Number of cells per relative [CM]: 1 = 82, 0.5 = 32, 0.3 = 29, 0.1 = 50, 0.001 = 29. Curves are fitted to log of concentration vs responses. Fits to the data gave an EC 50 of 0.38 for the normalized peak and 32 for the normalized area. The complete CM was considered 100, a dilution 1/10 is 10. EC_{50}: half-maximal effective concentration. (F) Traces showing transient changes in the $[Ca^{2+}]_i$ evoked by the CM in the presence or absence of 2 mM extracellular Ca^{2+}. (G) Box and whiskers plot showing the median normalized CM-evoked responses in the presence of Ca^{2+} and with no Ca^{2+} and 0.5 mM EGTA ($^{**}p = 0.0078$, for both comparisons $n = 8$ cells, two experiments; Wilcoxon test: $W = -36$, df = 7). (H) Two records from different neurons showing that CM exposure for more than 12 min, hinders calcium regulation after CM washout. (I) Two long consecutive exposures to CM, that together sum more than 12 min also impede calcium regulation. Traces with distinct colors correspond to responses of different neurons. (For interpretation of the references to colour in this figure legend, the reader is referred to the web version of this article.)

CM-evoked increase in $[Ca^{2+}]_i$. The magnitude of the MK-801 block was not the same for all neurons studied; such that in ~ 21% of the neurons the CM-mediated response was blocked between 0 and 25%, in ~ 37% of the neurons between 26 to 50%, in ~ 15% of the neurons between 51 and 75%, and in ~27% of the neurons between 76 and 100% ($n = 33$, $N = 2$ experiments). Even though the blockage level for some neurons was low when MK-801 was perfused along with CM, after the washout of CM plus MK-801, all responses produced by the second CM pulse were blocked (~78%, IQR = 61–89) (Fig. 5A-B), consistent with the mode of action of MK-801 (Huettner and Bean, 1988).

The CM effect was also studied in the presence of (2R)-amino-5-phosphonovaleric acid (AP-5) a reversible NMDAr inhibitor. In the initial experiments100 μM AP-5 appeared to have no effect on the CM-mediated response (data not shown). Since AP-5 is a competitive inhibitor, the experiments were repeated with a 10-fold dilution of the CM and the same AP-5 concentration. Fig. 5C-D shows the effect of the application of diluted CM by perfusion. When a steady $[Ca^{2+}]_i$ was reached with diluted CM, application of AP-5 blocked the CM-mediated $[Ca^{2+}]_i$ increase by 86.7% (IQR = 69 – 93). Block with AP-5 was fully reversible since the CM-evoked $[Ca^{2+}]_i$ increase was not significantly different before the AP-5 addition and after AP-5 washout ($p = 0.6830$) (Fig. 5D). AP-5 also blocked the evoked increase in $[Ca^{2+}]_i$ mediated by OpCM and SchwCM (data not shown).

Glycine is a co-agonist of NMDAr and in neuronal cultures endogenous glycine is usually present (Foster and Kemp, 1989; Courtney et al., 1990). To study whether the action of CM involved the glycine binding site, the effect of an antagonist that binds to the glycine site in the NMDAr, the (±) 3-Amino-1-hydroxy-pyrrolidin-2-one (HA-966) (Foster and Kemp, 1989; Courtney et al., 1990) was tested. When a steady response to the CM was achieved, application of HA-966 (200 μM) reduced the CM-evoked increase in $[Ca^{2+}]_i$ by 62.5%, and this block by HA-966 was fully reversible (IQR = 58–69; $n = 21$, CM vs HA-966 $p < 0.0001$ and CM vs CM wash $p = 0.9714$) (Fig. 5E, F). Moreover, application of glycine (10 μM glycine, 20 s pulse)

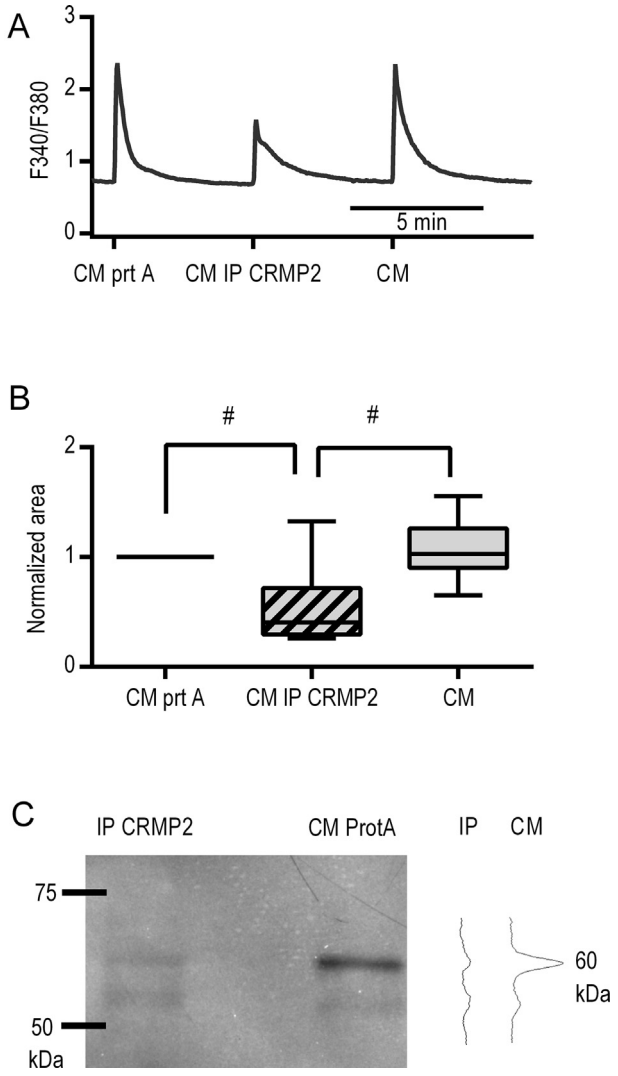

Fig. 3. Immunodepletion of CRMP2 from CM counteracts the CM-evoked $[Ca^{2+}]_i$ increase. (A) A representative trace illustrating the effect of immunodepleting CRMP2 from the CM. (B) Box and whiskers plot showing the normalized areas responses for cells treated with CM + protein A, CM immunodepleted from CRMP2 (IP CRMP2), and CM alone ($^{\#}p < 0.0001$, $n = 33$ neurons, 3 experiments, $H = 42.6$, 2 df; $n = 33$; $n = 3$ experiments Kruskal–Wallis with Dunn's post hoc test). (C) WB showing the resulting CRMP2 after being immunoprecipitated. On the right side, density profile showing the quantification of the CRMP-2 bands before (CM) and after IP.

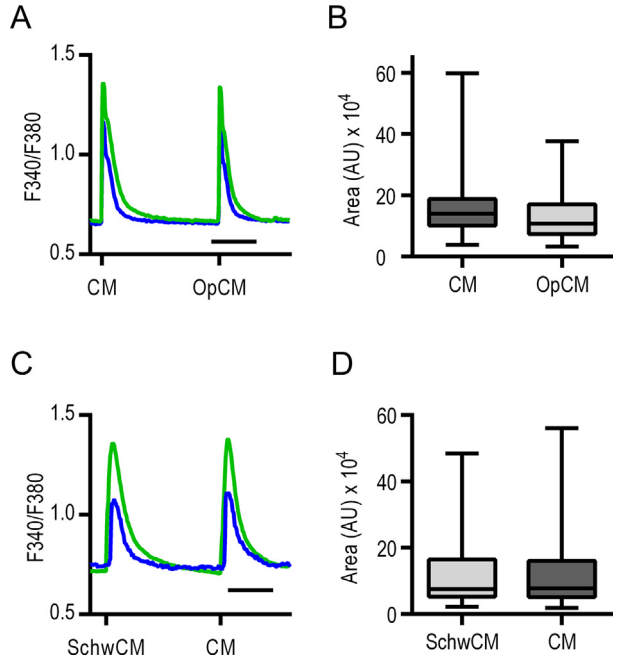

Fig. 4. Optic and Schwann cells CMs also increase $[Ca^{2+}]_i$. (A) Example traces of CM- and OpCM-evoked $[Ca^{2+}]_i$ increases. (B) Quantification shows the areas (AU) of Sciatic CM and optic CM ($n = 32$ cells, three experiments). (C) Example traces of Schw CM- and CM-evoked $[Ca^{2+}]_i$ increase. (D) Quantification of the areas (AU) of Schw CM and Sciatic CM responses ($n = 39$ cells, three experiments). Different color traces represent responses from distinct neurons. Scale bar = 2 min. (For interpretation of the references to color in this figure legend, the reader is referred to the web version of this article.)

displaced/reversed the HA-966 blocking effect. HA-966 blocked by 59% the CM-evoked $[Ca^{2+}]_i$ increase (IQR = 57–64) while glycine addition reversed HA-966 block (IQR = 114.8–130.5). The glycine effect in the presence of CM + HA-966 was similar to the effect of CM alone ($p = 0.6501$). These results indicate that CM may be acting in part through the glycine binding site in the NMDAr since it mimicked the effect of glycine on the NMDA-evoked $[Ca^{2+}]_i$ increase.

Another property of NMDAr is that they display Mg^{2+} voltage-dependent blockage (Paoletti, 2011). Hence, it was tested whether the CM-evoked $[Ca^{2+}]_i$ increase was blocked by Mg^{2+}, this was done by measuring the CM-evoked response in two different buffers, one containing Mg^{2+} (0.8 mM Mg^{2+} and 1.8 mM Ca^{2+}) and another without Mg^{2+} (0 Mg^{2+} and 2.6 mM Ca^{2+}). The overall concentration of divalent cations was the same in both buffers. Fig. 5-I shows a representative trace where consecutive CM pulses were applied; the first two CM pulses were applied in the presence of Mg^{2+}, the following two CM pulses were applied in the absence of Mg^{2+} and the last two CM pulses were applied again in the presence of Mg^{2+}. In the presence of Mg^{2+}, the first CM pulse induced a small increase in $[Ca^{2+}]_i$, while the second CM pulse induced a larger increase in $[Ca^{2+}]_i$ (3.1 times; $p < 0.0001$, median first pulse = 0.35, IQR-0.27 – 0.39; median second pulse 1.07, IQR = 0.8 – 1.45) (Fig. 5I-J). The subsequent two pulses done in the absence of Mg^{2+}, evoked large increases in $[Ca^{2+}]_i$ of similar magnitude. Reintroduction of Mg^{2+} reduced the first CM-evoked response by 6.1-fold ($p < 0.0001$, median of pulse with Mg^{2+} = 0.79, IQR = 0.74 – 0.83; first pulse without Mg^{2+} = 0.13, IQR = 0.08 – 0.19). The second CM-pulse following reintroduction of Mg^{2+} again produced a larger response 5.2-fold larger as compared with the first one ($p < 0.0001$, median second pulse with Mg^{2+} = 0.68, IQR = 0.54 – 0.88). These results suggest that application of CM may depolarize the cells which would reduce Mg^{2+} blockage of NMDAr allowing an increase in the CM-evoked response upon repetitive CM applications in the presence of Mg^{2+}. The magnitude of

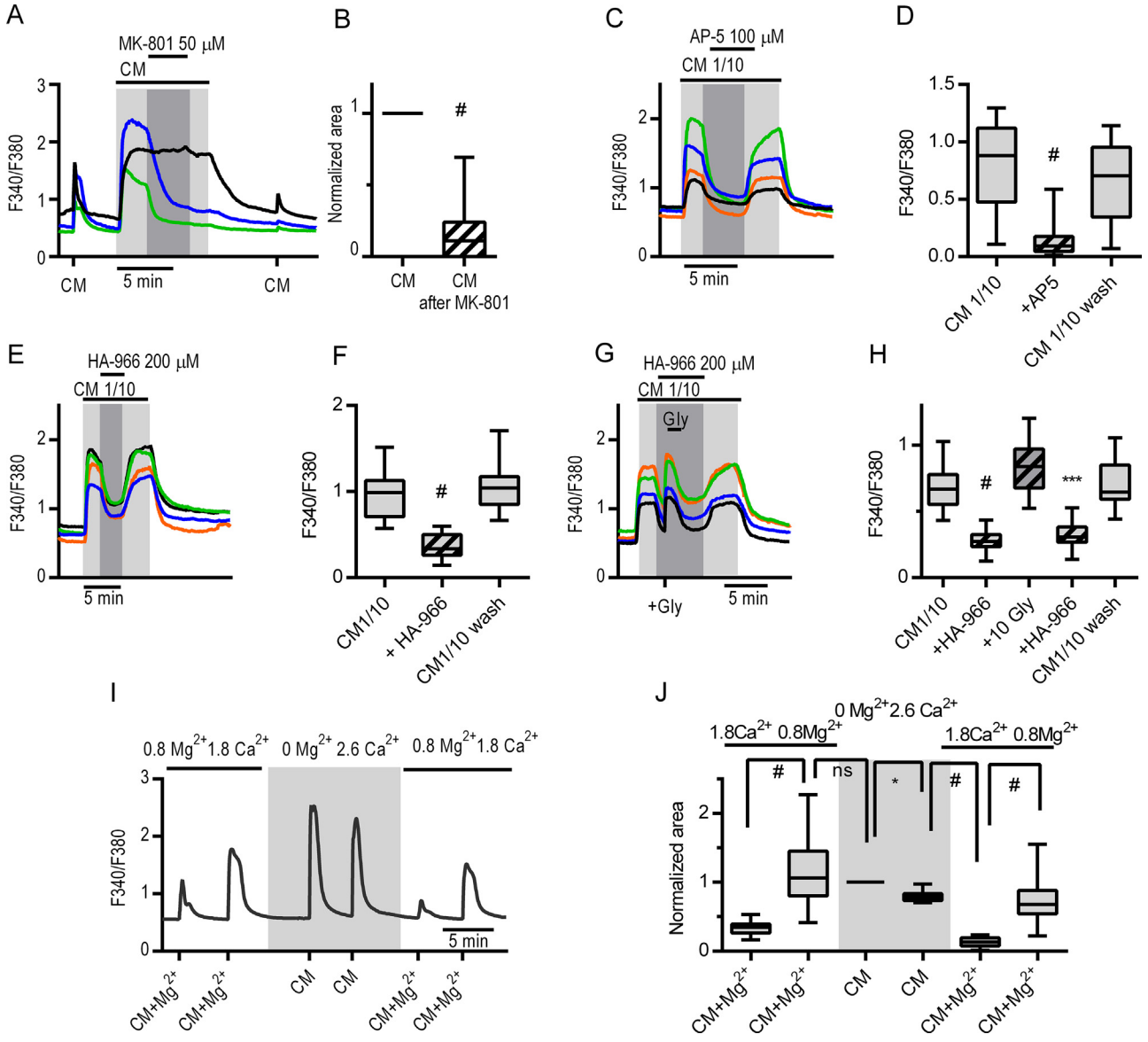

Fig. 5. CM-evoked $[Ca^{2+}]_i$ increase is blocked by NMDAr antagonists. (A) Fura-2 ratio variation when CM was applied continuously and MK-801 applied subsequently (33 neurons, 2 experiments). (B) Box and whiskers plot representing normalized median $[Ca^{2+}]_i$ increase of CM pulses applied before and after MK-801 inhibition. The CM pulse applied after perfusion with MK-801 remained blocked (*) (# = $p < 0.0001$; $n = 30$ neurons; two experiments; Wilcoxon test W = −465, df = 29). (C) Fura-2 ratio changes when a diluted CM (1/10) was applied continuously and AP-5 100 μM applied subsequently and then removed. (D) Box and whiskers plot of the ratios (measured at steady state) from traces shown in (C) (# $p < 0.0001$, $n = 21$; Kruskal–Wallis $H = 32.09$, df = 2 with Dunn's post hoc test). (E) Representative traces of $[Ca^{2+}]_i$ increase when CM was applied continuously and HA-966 200 μM was co-applied and then removed. (F) Quantification of ratios shown in (E) ($p < 0.0001$, $n = 20$; Kruskal–Wallis $H = 39.63$, df = 2, with post hoc Dunn's test). (G) Representative traces of $[Ca^{2+}]_i$ changes showing the effect of a 20 s glycine pulse (10 μM) when CM 1/10 was applied continuously with HA-966 200 μM. (H) Quantification of ratios shown in (G) ($^{\#}p < 0.0001$; $^{***}p = 0.0002$, $n = 17$; Kruskal–Wallis $H = 60.69$, df = 4 with Dunn's post hoc test). (I) Effect of Mg^{2+} on the evoked-$[Ca^{2+}]_i$. Example trace of Fura-2 ratio changes of CM-evoked transient calcium increases in the presence or absence of 0.8 mM Mg^{2+} (gray shaded area indicates Mg^{2+} free solution). Scale bar = 5 min. Values were normalized to the first pulse with 0 Mg^{2+} buffer. (J) Box and whiskers graph showing the median normalized CM-evoked responses (area of the transient increase in $[Ca^{2+}]_i$) in absence (plain boxes) and presence of Mg^{2+} (hatched boxes). For each cell, the CM-evoked increase was normalized to the first pulse in 0 Mg^{2+}. Note that the first response in the presence of Mg^{2+} is attenuated compared to the obtained in the absence of Mg^{2+} ($^*p = 0.0130$, $^{\#}p < 0.0001$; $n = 30$ cells, two experiments; Kruskal–Wallis $H = 140.9$, df = 5 with Dunn's post hoc test). Light gray shaded area represents when CM was being perfused and dark gray shaded area when the antagonist was present together with the CM. Distinct color traces correspond to different neuron responses under the condition stated in each panel. (For interpretation of the references to colour in this figure legend, the reader is referred to the web version of this article.)

the CM-evoked responses in the presence of 1.8 mM or 2.6 mM Ca^{2+} was similar. The responses obtained when CM was applied in the presence of 1.8 mM Ca^{2+} had a median of 30.5 arbitrary units (au) (IQR = 25.1–35.7), and when applied in the presence of 2.6 mM Ca^{2+} it had a median of 37 au (IQR = 24.5–37.9; $n = 11$; $p = 0.4385$ $U = 48$, df = 10, Mann–Whitney test). The Mg^{2+} dependence of the CM-evoked response

(Fig. 5I, J) were consistent with NMDAr mediating the CM-evoked increase in $[Ca^{2+}]_i$.

Mode of action of CM on the NMDAr binding sites

The above experiments with glutamate receptor antagonists and Mg^{2+} supported the involvement of the NMDArs in the CM-mediated increase in $[Ca^{2+}]_i$. Next, it was investigated whether CM was acting through actions on the NMDAr agonist binding sites. This was done by perfusing CM alone and with an NMDAr agonist (NMDA or glycine). Addition of NMDA following exposure to CM did not produce an additional change in the $[Ca^{2+}]_i$ levels. However, addition of CM following exposure to NMDA produced an additional increase in the $[Ca^{2+}]_i$ levels (Fig. 6B). In a similar manner, addition of glycine (10 μM) following exposure to NMDA produced an additional increase in the $[Ca^{2+}]_i$ levels (Fig. 6C), as previously reported (Johnson and Ascher, 1987). Ratios were calculated for every application and the values are shown in Fig. 6D (CM/CM = 1.04, IQR = 1.002–1.009, n = 25; N = 2 experiments; CM + NMDA/CM = 0.96, IQR = 0.91–1.02; n = 34; N = 2 experiments, Fig. 6A; NMDA + CM/NMDA = 1.67, IQR = 1.54–1.99; n = 60, N = 3 experiments, Fig. 6B; NMDA + Gly/NMDA = 1.69, IQR = 1.4–1.94; n = 68, N = 4 experiments, Fig. 6C). Therefore, values obtained for NMDA + Gly/NMDA *vs* NMDA + CM/NMDA were similar (p > 0.9999) suggesting that CM enhanced the NMDA evoked $[Ca^{2+}]_i$ increase in a similar way as glycine does.

Effect of CM on neurotransmitter release

Due to the effect of CM on the binding sites for the NMDAr agonist, we investigated whether CM had an effect on glutamate and glycine release. Indeed, CM application increased the concentration of glutamate (values were subtracted from controls) (median = 9.7 μM, IQR = 6.8–18.4, n = 6 experiments) and glycine (median = 17.4 μM, IQR = 0.83–28.4, n = 3 experiments) in the extracellular media. Control measurements of CM revealed that the CM was free of glutamate and glycine (n = 3 experiments). The CM-evoked release of glutamate and glycine is consistent with the observed CM-mediated potentiation of the NMDA response (Fig. 6B). Release of glutamate and glycine has also been reported for cortical neurons exposed to NMDA (López et al., 2010).

CRMP2 is responsible for the $[Ca^{2+}]_i$ increase via extracellular NMDAr activation

CRMP2 has been implicated in the intracellular regulation of NMDAr and N-type VDCC (Brittain et al., 2009, 2011b, 2012; Brustovetsky et al., 2014). Having identified CRMP2 in the CM, we studied if this protein could be responsible for the CM-evoked $[Ca^{2+}]_i$ increase. CBD3 is a peptide derived from CRMP2 and it is conjugated to HIV transduction domain protein tat (tat-CBD3) to facilitate penetration to the cell. CBD3 interferes with the intracellular CRMP2-NMDAr interaction, and reduces the NMDA-evoked $[Ca^{2+}]_i$ increase (Brittain et al., 2009; Brustovetsky et al., 2014; Moutal et al., 2015). We tested whether tat-CBD3 could affect the CRMP2-CM-evoked $[Ca^{2+}]_i$ increase. Fig. 7A, shows a representative trace of CM and NMDA-evoked $[Ca^{2+}]_i$ increase before, during and after perfusion of 5 μM tat-CBD3 peptide. Tat-CBD3 decreased the CM-evoked response to 61.8% (IQR = 50–74) and 75.9% (IQR = 54–84) for areas and peaks, respectively. Tat-CBD3 decreased the NMDA evoked response to 46.2% (IQR = 41–58) and 31.9% (IQR = 22–41) for areas and peaks, respectively (n = 28; N = 2 experiments) (Fig. 7B) as previously reported (Brustovetsky et al. 2014).

Previously, it was shown that perfusion of tat-CBD3 for 5 min

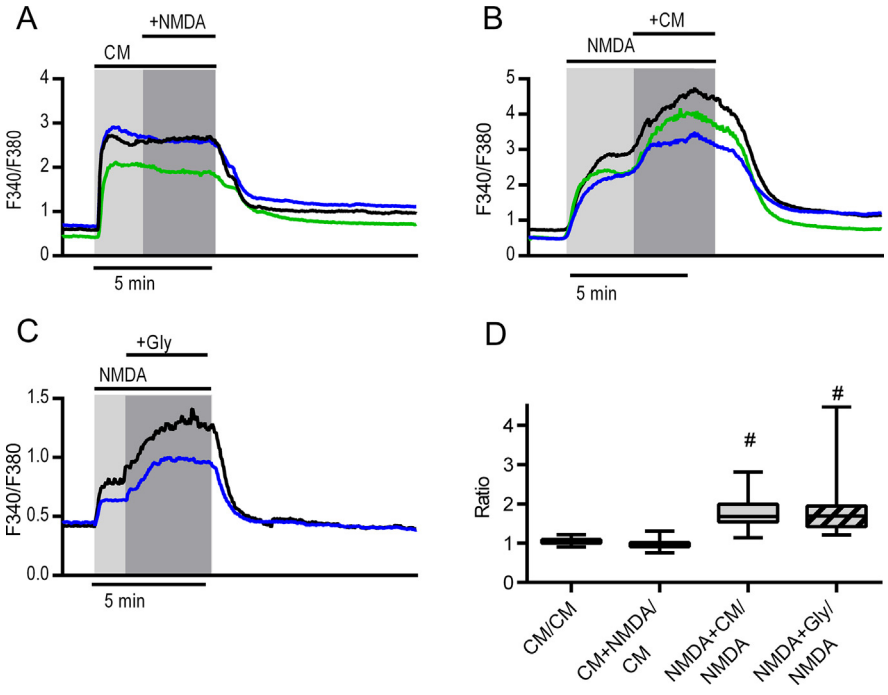

Fig. 6. Mode of action of CM on the NMDAr binding sites. (A) Examples of traces obtained when CM was perfused for several minutes (light gray shaded area) and NMDA was applied while CM was present (dark gray shaded area). (B) Traces obtained when NMDA was perfused (light gray shaded area) and then CM was applied together with NMDA (dark gray shaded area). (C) Traces obtained when NMDA was perfused (light gray shaded area) and then glycine 10 μM was applied together with NMDA (dark gray shaded area). (D) Box and whiskers plot representing the ratios obtained when dividing the second agonist over the first one: CM/CM n = 25; CM + NMDA/CM n = 34; NMDA + CM/NMDA n = 60; NMDA + Gly/NMDA n = 68; Kruskal–Wallis analysis H = 120.6, df = 3, with Dunn's multiple comparison test of each column vs CM/CM, # p < 0.0001. Distinct color traces correspond to different neuron responses under the condition stated in each panel. (For interpretation of the references to colour in this figure legend, the reader is referred to the web version of this article.)

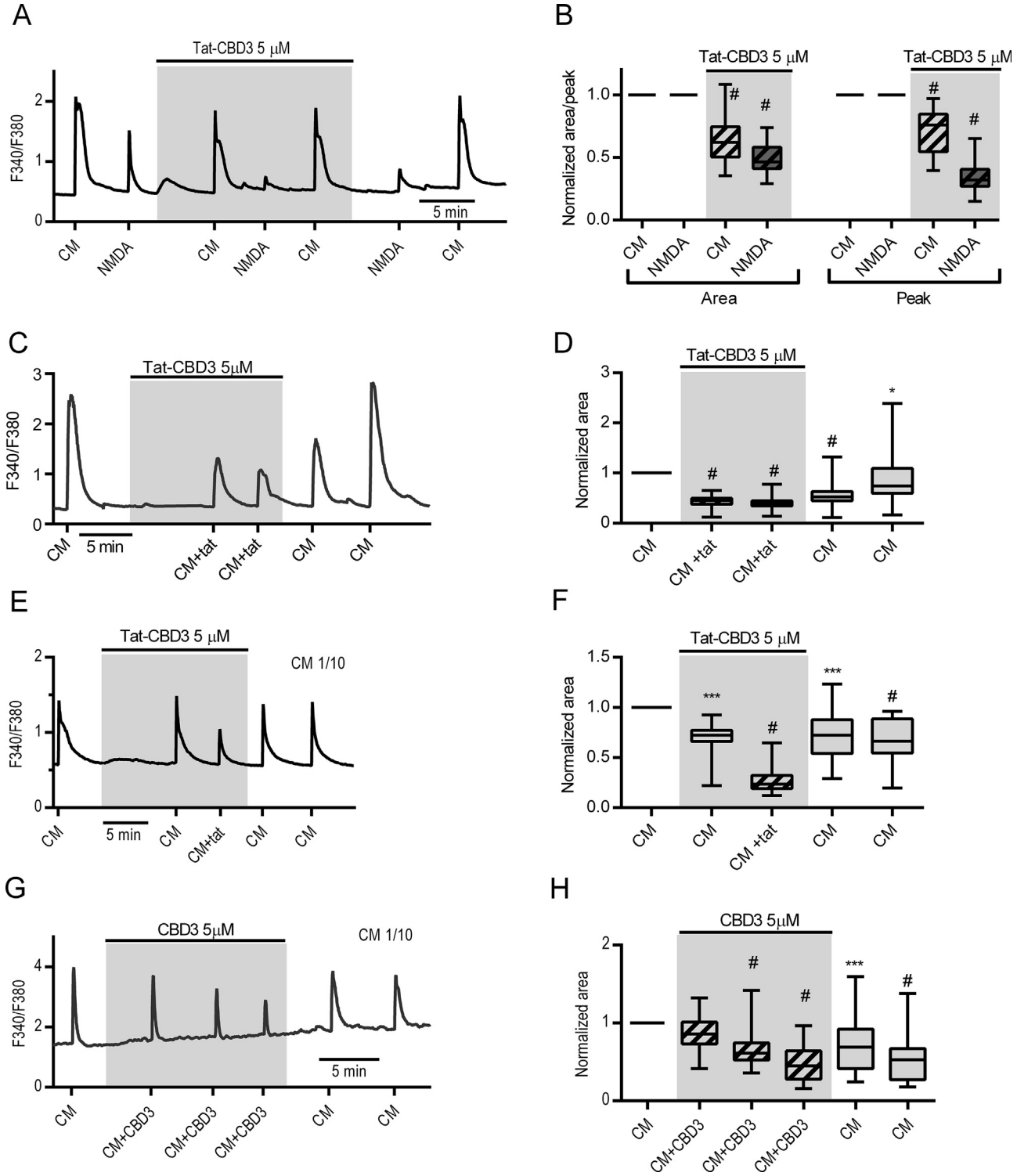

Fig. 7. Effect of a CRMP2 neuroprotective peptide (tat-CBD3) on CM- and NMDA-evoked $[Ca^{2+}]_i$ increase. (A) A representative trace of the CM and NMDA-evoked $[Ca^{2+}]_i$ increase before, during and after perfusion with tat-CBD3 peptide. (B) Graph showing the normalized areas and peaks of the CM and NMDA-evoked calcium increase, normalized to the first response of the respective CM or NMDA application ($^{\#}p < 0.0001$; $n = 28$ cells from two experiments; Wilcoxon test W_{area} CM $= -402$, df $= 27$; W_{peak} CM $= -406$ df $= 27$; W_{NMDA} area $W = -406$, df $= 27$; W_{NMDA} peak $= -406$ df $= 27$). (C) Effect of the focal application of CM + tat-CBD3 during perfusion with tat-CBD3. (D) Quantification of the effect shown in C depicting the normalized areas obtained under each condition ($^{\#}p < 0.0001$, $^{*}p = 0.0333$ $n = 47$, three experiments; Kruskal–Wallis $H = 137$ df $= 4$, with Dunn's post hoc test). (E) Effect of CM diluted 1/10 when applied together with tat-CBD3. F. Normalized areas of responses shown in (E) ($^{***}p = 0.0004$, $^{\#}p < 0.0001$, $^{***}p = 0.0007$, $^{\#}p < 0.0001$, $n = 18$; Kruskal–Wallis $H = 58.77$ df $= 4$ with Dunn's post hoc test). Shaded rectangles indicate when tat-CBD3 was being perfused. (G) Effect of CM diluted 1/10 when applied together with CBD3 peptide. (H) Normalized areas from responses shown in G (ns $p = 0.2101$, $^{\#}p < 0.0001$ and $^{***}p = 0.0007$, $n = 27$, three experiments, Kruskal–Wallis $H = 62.82$ df $= 5$ with Dunn's post hoc test).

before applying an NMDA-pulse (without tat-CBD3) was sufficient to decrease on the NMDA-evoked $[Ca^{2+}]_i$ increase, suggesting that tat-CBD3 was acting intracellularly (Brittain et al. 2011). Hence, whether or not tat-CBD3 was acting extracellularly to decrease the CM response, tat-CBD3 was applied in the perfusion and the CM pulse with or without the tat-CBD3 peptide. When tat-CBD3 was present in the CM-pulse, the CM-evoked $[Ca^{2+}]_i$ increase was reduced to 45.1% (IQR = 38–50) for the first CM + tat-CBD3 pulse, and to 38.7% (IQR = 34–44) for the second CM + tat-CBD3 pulse (Fig. 7C). After washout of tat-CBD3, the effect on the CM-evoked $[Ca^{2+}]_i$ increase was reversed and displayed a progressive recovery, first to 52% (IQR = 44–63) and then to 75.9% (IQR = 60–110; n = 47; 3 experiments) for the first and second CM pulse following tat-CBD3 washout (Fig. 7C, D). In contrast, following 5-min perfusion with tat-CBD3, when the CM pulse was done in the absence of tat-CBD3, the CM response was only slightly reduced to 72.2% (IQR = 66–77), and in the same experiment when CM was applied in the presence of tat-CBD3 the CM response decreased to 23.6% (IQR = 19–32). Removal of tat-CBD3 restored the CM response to 72.5% (IQR = 55–88) (Fig. 7F). These results show that, in order to block the CM-evoked $[Ca^{2+}]_i$ increase, it was necessary to add tat-CBD3 not only to the perfusion but also to the CM-pulse suggesting that tat-CBD3 may be acting extracellularly to reduce the CM-response.

The above results suggested that CRMP2-CM could be acting from the extracellular side. To corroborate this possibility, the non-permeable CBD3 peptide (Brittain et al., 2011b) was also used. Fig. 7G shows that the presence of CBD3 (5 μM) also produced a progressive decrease in the CM response, and that this CBD3 action was reversible upon washout. Fig. 7H shows the normalized quantification of the traces shown in 7G; the first CM pulse with CBD3 decreased to 86% (IQR = 73–100, p = 0.2101), the second pulse response decreased to 61% (IQR = 52–74; $p < 0.0001$), the third pulse decreased to 49% (IQR = 27–64; n = 27), $p < 0.0001$, and after CBD3 peptide washout, the CM response recovered to 69% (IQR = 41–92; n = 27), p = 0.0005 (three experiments). Together, these results confirm that CBD3 peptide is able to decrease the CRMP2-CM evoked- $[Ca^{2+}]_i$ increase by acting on the extracellular side.

N-type VDCCss are also involved in the CM effect

The above results indicate that the CM-evoked $[Ca^{2+}_{ji}$ increase was mainly mediated through actions on the NMDAr. However, NMDAr blockers (MK-801 and AP-5) did not fully block the CM response (Fig. 5A–D, Fig. 8F), in the presence of NMDAr blockers the CM still evoked a small $[Ca^{2+}]$ increase (≈13%). Hence, various blockers were tested to identify whether other channels/receptors could be contributing to the CM response. Nifedipine (5 μM), an L-type VDCC antagonist, did not significantly affect the CM-evoked $[Ca^{2+}]_i$ increase (Fig. 8F). However, ω-conotoxin GVIA (1–2.5 μM), an N-type VDCC inhibitor, decreased the CM-evoked response by 33% (IQR = 24–46; n = 21; Fig. 8A, B). Moreover, in experiments were CM was perfused by itself or together with ω-conotoxin-GVIA and the data was normalized to the initial KCl-evoked response, the median ratio was 2.92 (IQR = 2.2–4.8; n = 22; two experiments), while the ratio of CM + ω-conotoxin–GVIA/KCl was 1.76 (IQR = 1.4–2.7, n = 20, two experiments) (Fig. 8C–E). These results suggest that ω-conotoxin-GVIA inhibited ≈40% of the CM-evoked $[Ca^{2+}]_i$ increase. When ω-conotoxin-GVIA was perfused 5 min before CM + ω-conotoxin-GVIA, no further decrease was obtained (data not shown). These results indicate that N-type VDCCs are also involved in the CM-evoked $[Ca^{2+}]_i$ increase. Interestingly, the percentage of decrease of the CM response with the N-type VDCC blocker was larger (∼33% block) than the residual CM response following block with NMDAr antagonist AP-5 (∼13% residual). It is known that activation of N-type VDCC induced glutamate release (Scholz and Miller, 1995); and here it was shown that CM also induced glutamate release. Hence, the inhibitory action of ω-conotoxin-GVIA on the CM response may result from blocking the N-type VDCC and glutamate release.

Lastly, the contribution of other glutamate receptors like AMPA and Kainate receptors was assessed. CNQX (6-cyano-7-nitroquinoxaline-2,3-dione) (200 μM) a competitive AMPA/kainate receptor antagonist decreased the CM-evoked $[Ca^{2+}]_i$ increase by 19.6% (IQR = 15–25; n = 17, two experiments) (Fig. 8F). This block, although significant, it was smaller than that observed when using NMDAr antagonists, and were consistent with the measured CM-evoked glutamate release. Altogether, these results suggest that the $[Ca^{2+}]_i$ increase occurs mostly through direct actions on the NMDAr, and through indirect actions of N-type VDCC that promote glutamate release.

CRMP2 from CM binds to the external plasma membrane and affects neurite integrity

Some of the above shown functional studies indicated that the CRMP2-CM-evoked $[Ca^{2+}]_i$ increase was mediated by an extracellular interaction. To further investigate this possibility double labeling with anti-CRMP2 antibody and the surface membrane marker (WGA-A488) was done using live hippocampal cells. Live cells were used to avoid the internalization of the antibody. In the absence of CM, anti-CRMP2 antibody did not label live hippocampal cells (Fig. 9A top panels). Live hippocampal cells exposed to both CM and anti-CRMP2 antibody displayed CRMP2-labeling (red) that co-localized with the surface membrane marker WGA-A488 (green) (Fig. 9A, middle panels), indicating that CRMP2-CM interacted with extracellular membranes sites. In fixed hippocampal cells, (in the absence of CM) the anti-CRMP2 antibody labeled endogenous CRMP2 (Fig. 9A, bottom panels). The pattern of labeling for the endogenous CRMP2 was different to that of external CRMP2-CM. Quantification of the overlap labeling of exogenous CRMP2 with the membrane surface marker WGA-A488, showed a good correlation as indicated by the Pearson's coefficient (median = 0.85, IQR = 0.69–0.89; n = 50; N = 3 experiments, Fig. 9B). On the other hand, the labeling of endogenous CRMP2 with the membrane surface marker showed a poor correlation,

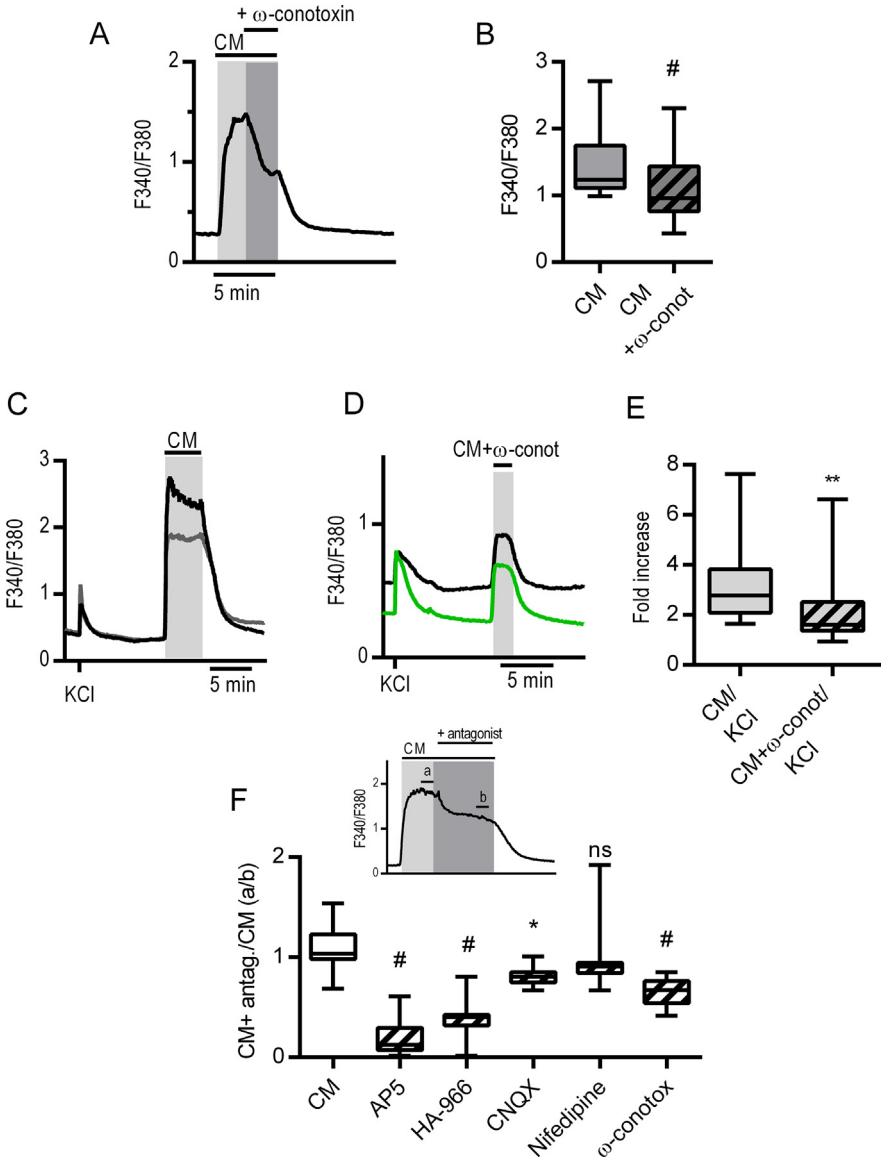

Fig. 8. Effect of ω-conotoxin GVIA when applied by perfusion. (A) Example trace of CM and addition of ω-conotoxin GVIA (1 μM) after CM reached a plateau (dark gray area). (B) Box and whiskers graph depicting the quantification of the results shown in (A) ($^{**}p$ = 0.004, n = 25 cells, three experiments; Mann Whitney U = 166). (C) Example traces of a KCl pulse and CM applied by perfusion. (D) Example traces showing a KCl pulse and CM + 1 μM ω-conotoxin GVIA applied by perfusion. (E) Box and whiskers graph depicting the ratio between the KCl peak and the CM peak without (shown in (C)) or with 1 μM ω-conotoxin GVIA (shown in (D)) ($^{**}p$ = 0.0006, nCM = 24, nCM + ω-conotoxi$n$ = 19 cells, three experiments; Mann Whitney U = 92). These experiments were done in different cells because when two long CM pulses were applied, the response to the second pulse was always smaller than the first one. (F) Graph depicting the effect of different antagonists on the CM-evoked $[Ca^{2+}]_i$ increase. Values were obtained by dividing the mean value at the steady state after the application of CM with the antagonist (b) by the mean maximal value obtained with CM alone (a) (inset figure). Comparisons were made against CM (n = 32, four experiments; AP5 $p < 0.0001$, n = 22, one experiment; HA-966$p < 0.0001$, n = 38, two experiments; CNQX $^{*}p$ = 0.039, n = 17, two experiments; nifedipine p = 0.8028, n = 18, two experiments; and ω-conotoxin-GVIA $p < 0.000$, n = 21, four experiments). Distinct color traces correspond to different neuron responses under the condition stated in each panel. (For interpretation of the references to colour in this figure legend, the reader is referred to the web version of this article.)

as indicated by a very low Pearson's coefficient (median = 0.33; IQR = 0.12–0.49; n = 32; N = 3 experiments Fig. 9B, C). These results show that CRMP2 is capable of binding to molecules on the cell membrane surface. Additionally, we observed that 30 min exposure to CM affected neurite integrity and CRMP2 and MAP2 labeling changed from control (NB) to CM as shown in Fig. 9D (middle bottom panel). At least 6 experiments were done and in all experiments the fragmented labeling was observed. Fig. 9D shows confocal images of cells exposed either to CM or NB. In the case of CM, as in the first experiments, neurons were simultaneously labeled with CRMP2 antibody and then fixed and immunostained with MAP2 antibody to label neurons and dendrites; while for NB-treated cells, these were fixed and double-labeled with CRMP2 and MAP2. Neurons treated with NB show a continuous labeling for MAP2 and CRMP2 indicating that their neurites were healthy (Fig. 9D top panels). On the other hand, neurons exposed to CM show a fragmented labeling for both markers, observing neurites with a patchy labeling as compared to neurons in NB (Fig. 9D, bottom panels). A similar finding was reported by Hou et al. (2009); where exposure to glutamate for an extended period of time induced dendrite and axon stress manifested as varicosities and axon fragmentation (Hou et al., 2009) that ended in neuronal death (Hou et al., 2006).

Recombinant CRMP2 also evokes $[Ca^{2+}]_i$ increase via NMDAr activation

All the evidence suggests that CRMP2 is the protein responsible for the CM-evoked $[Ca^{2+}]_i$ increase. To further confirm this, mouse recombinant CRMP2 (rCRMP2) was tested on hippocampal neurons. Fig. 10A, B show that focal application (rapid application) of rCRMP2 produced a concentration-dependent increase in $[Ca^{2+}]_i$ in hippocampal neurons. Fig. 10E–F show that if the time of application was increased from 2 s to 4 s, the response increased 1.6-fold (IQR = 1.4–2.6), and when 6 s were applied, the response increased 2.9-fold (IQR = 2.7–4.5, n = 15, two experiments). When comparing the consecutive pulse application of CM (Fig. 2A, B) to the consecutive pulse application of rCRMP2 (Fig. 10C, D), the evoked Ca^{2+} increase diminished further with the number of pulses applied,

indicating a higher level of NMDAr desensitization when rCRPM2 was applied.

When CM was applied by perfusion, the response remained strong (Fig. 2C), but when rCRMP2 was applied by perfusion, the response was very small (Fig. 10G) (25 out of 56 neurons responded to rCRMP2, four experiments), suggesting that there may be something else in the CM that may be stabilizing the action of CRMP2 in the CM. Both, the reversible NMDAr blocker AP-5 (Fig. 10H, I) and irreversible NMDAr blocker MK-801 (Fig. 10J, K), blocked the rCRMP2-evoked $[Ca^{2+}]_i$ increase; confirming that the rCRMP2 response was mediated through the NMDAr.

Finally, to investigate the possibility that rCRMP2 could directly bind to the extracellular region of the NMDAr, an *in silico* study was done using the docking program CABSdock server. The CBD3 peptide (C-terminal side of CRMP2; Fig. 11B) was tested against the extracellular regions of the NMDAr (Fig. 11A). CABSdock generated 10 possible binding sites for the CBD3 peptide on its extracellular domain. Fig. 11A shows the best ranked binding site for each case. These results strongly indicate that it is possible that CRMP2 could activate this protein by direct binding to its extracellular side. Albeit the docking was performed with the CBD3 peptide (15 aa), there seems to be no

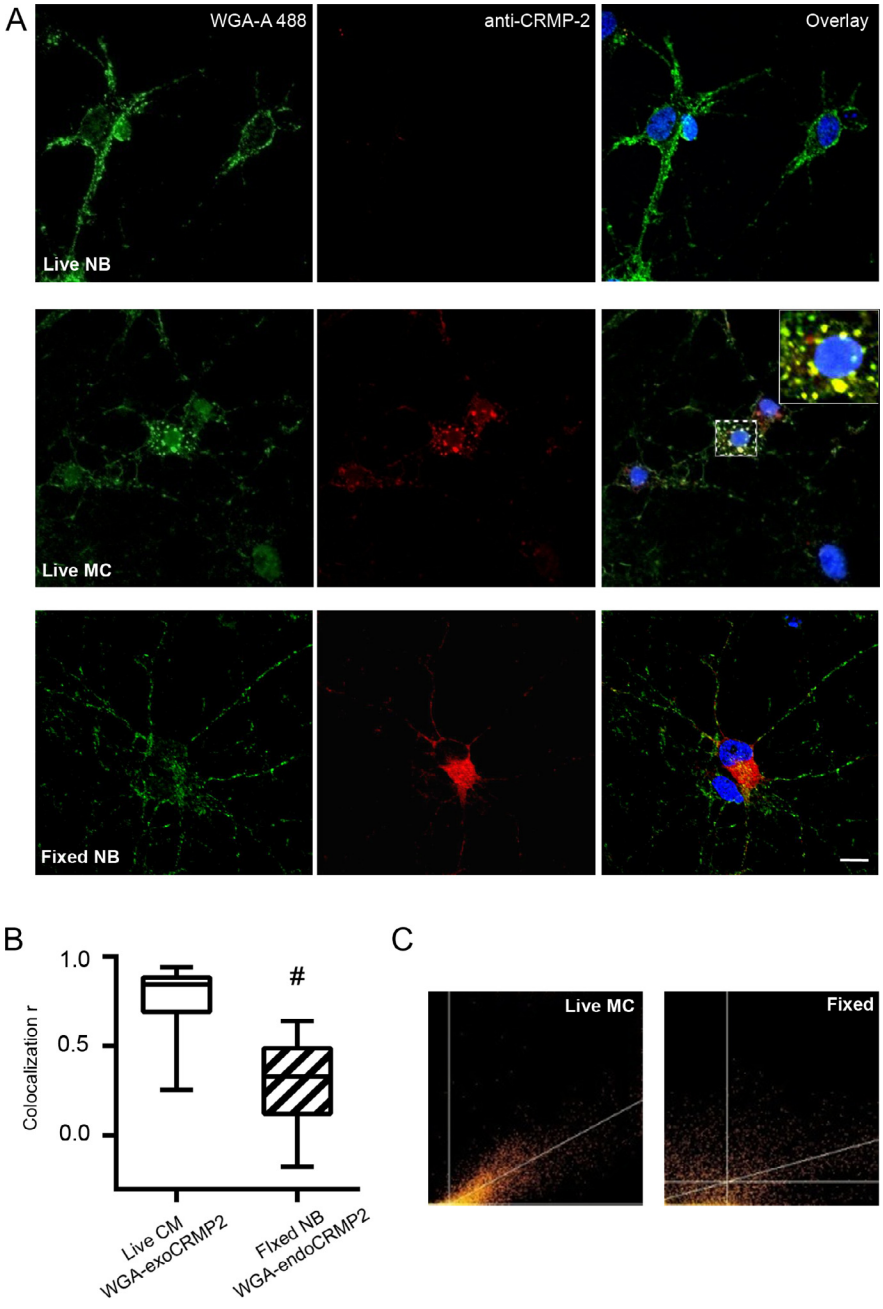

Fig. 9. CRMP2 from CM binds to the plasma membrane surface in hippocampal neurons. (A) Immunofluorescence micrographs of hippocampal neurons incubated with the plasma membrane marker (WGA-A 488) and the anti-CRMP2 antibody. Live cells were incubated with neurobasal medium (NB) and no CRMP2 signal was detected (upper micrographs, middle panel). When live cells were incubated with the CM, a specific signal from the exogenous CRMP2 labeling the plasma membrane was observed (middle micrographs, red, middle panels), which overlapped with the membrane marker WA-A488 (Green and overlay, middle panels). This overlap is better appreciated in the enlarged region showed in the inset. The bottom micrographs show the endogenous CRMP2 in cells grown in NB and then fixed. The intracellular distribution of this cytoplasmic protein (red) can be observed and there is no overlapping between CRMP2 and WGA-A488. Scale bar = 10 μm. (B) Box and whiskers plot showing the quantification of the extent of co-localization between the exogenous CRMP2 and WGA-A488 in live cells incubated with CM (Live-CM) and the endogenous CRMP2 in fixed cells incubated in NB (Fixed-NB). The Pearson's correlation coefficient (r) was determined using Image J ($^{\#}p < 0.0001$, Live CM $n = 50$; Fixed NB $n = 32$, three experiments; Mann Whitney test $U = 118$). (C) Representative scatter plots from the quantification of the co-localization between CRMP2 and WGA-A488 of Live CM and fixed NB. (D) CM affects neurite integrity. Immunofluorescence micrographs of hippocampal neurons immunolabeled with anti-MAP2 antibody (green) and anti-CRMP2 antibody (red). Live cells treated with NB (top panels) or CM (bottom panels) for 30 min. Neurons exposed to CM showed fragmented neurites indicative of neuron damage. Scale bar = 10 μm. In the insets of the overlay are shown an enlargement of a sections the neurites showing the fragmentation when exposed to CM. At least six experiments were done with the anti-CRMP2 antibody and two experiments with anti-MAP2 and anti-CRMP2. (For interpretation of the references to color in this figure legend, the reader is referred to the web version of this article.)

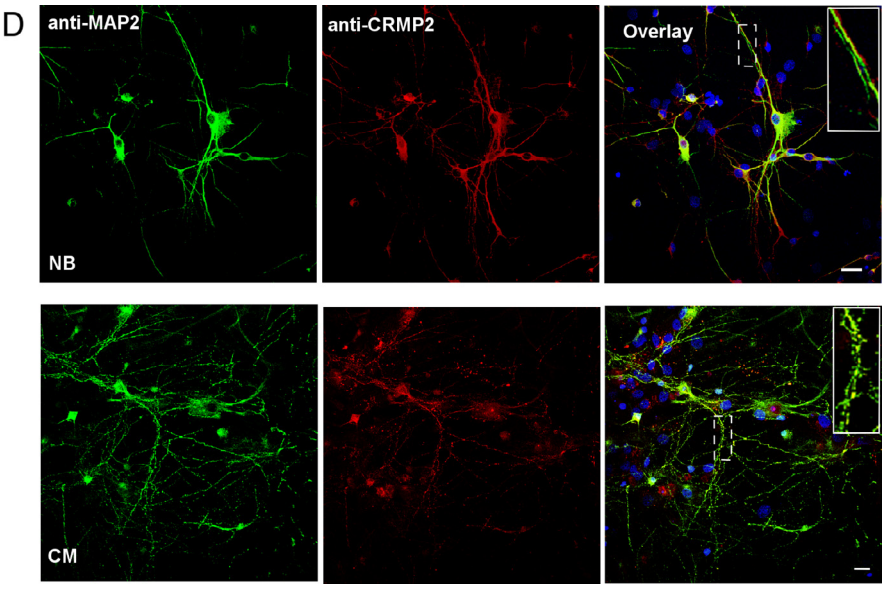

Fig. 9 (*continued*)

steric hindrance for the whole CRMP2 molecule to fit in those regions where the peptide is binding.

DISCUSSION

In this study, we demonstrate that extracellular application of CMs from sciatic nerves, optic nerves and Schwann cell cultures evoke $[Ca^{2+}]_i$ increase through actions on the NMDAr. This finding is based in the following results: (i) the response was dependent on extracellular calcium; (ii) specific NMDAr antagonists: MK-801 (non-competitive antagonist), AP-5 (competitive antagonist acting on the glutamate site) and HA-966 (acts on the glycine site) blocked the CM-evoked $[Ca^{2+}]_i$ increase; and (iii), Mg^{2+} (a voltage-dependent blocker of the ligand binding to the NMDAr) also blocked the CM-evoked $[Ca^{2+}]_i$ increase.

The identification of CRMP2 in the CM and the observation that CRMP2 immunoprecipitation decreased the CM-evoked response, suggested that CRMP2 was implicated in the observed CM-evoked Ca^{2+} increase. To validate this result, tat-CBD3 and CBD3 peptides were used. Tat-CBD3 is known to block the intracellular interaction of CRMP2 with NMDAr and VDCC (Brittain et al., 2011a, 2012; Brustovetsky et al., 2014), and the CBD3 peptide is not able to cross the cytoplasmic membrane (Brittain et al., 2011a). A key finding of this work is that these peptides diminished the CM-evoked $[Ca^{2+}]_i$ increase, probably by interfering with the binding of CRMP2 to the NMDAr. In addition, the immunolabeling with CRMP-2 antibody of live neurons also supported that CRMP2 can bind to the extracellular membrane. Finally, it was found that extracellular application of recombinant CRMP2 (rCRMP2) also evoked a $[Ca^{2+}]_i$ increase. It was found that rCRMP2 evoked $[Ca^{2+}]_i$ in a concentration-dependent manner when applied focally, but when it was applied by perfusion the effect was transient and smaller. Further studies will be necessary to elucidate the difference in the apparent rate of desensitization between the CM- and the rCRMP2-evoked $[Ca^{2+}]_i$ increase. However, one possible explanation is that in hippocampal neurons, NMDAr activation by rCRMP2 results in a fast desensitization of NMDAr, suggesting that the CM may have an additional molecule that slows down desensitization when this receptor is activated by CRMP2. We must also consider the possibility that another molecule in the CM induces glycine liberation that slows down desensitization (Lerma et al., 1990; Lester and Jahr, 1992). The desensitization of NMDAr during the application of rCRMP2 could be due to a small increase of intracellular calcium that would favor the activity of calcineurin promoting the desensitization of the receptors because CAMKII will not be activated and hence, it will not phosphorylate NMDAr to maintain its activity. This affirmation is based on experiments where the amount of intracellular calcium switches between calcineurin and CAMKII (Wen et al., 2004). Since CRMP2 is present in various CMs, including injured nerves (sciatic and optic nerves) and cultured Schwann cells, it suggests that CRMP2 may be secreted and may exert its extracellular action in normal as well as in nerve-injured states. In this sense, a growing number of observations indicates that CRMP2 is secreted. CRMP2 has been found in cancer secretomes (Wu et al., 2008) and in conditioned media of several cell lines (Brown et al., 2013). CRMP2 peptides have also been detected in cerebrospinal fluid from healthy individuals (Schutzer et al., 2010; Chiasserini et al., 2014), in patients with neurological disorders (Menon et al., 2011; Zhang et al., 2015a,b; Kroksveen et al., 2017) and in plasma samples from patients with severe trauma (Liu et al., 2006). There is evidence that CRMP2 is released to the extracellular milieu through exosomes formed by budding of endosomal membrane. (Prudovsky et al., 2008; Schneider and Simons, 2013; Levy, 2017). CRMP2 has been identified *in vitro* in exosomes (both protein and mRNA forms) derived from cancer and normal human tissue (Vesiclepedia: http://www.microvesicles.org/; Exocarta: http://www.exocarta.org/); and from mouse and rat cells (Cortazar et al., 2017).

Until now, CRMP2 has been described as a cytosolic protein that interacts with NMDAr and VDCC at the intracellular level. The intracellular interactions between N-type VDCC and CRMP2 has been studied in neurons by transfecting or by knocking down CRMP2. Neurons that overexpress CRMP2 display an increase in voltage-dependent Ca^{2+} currents and neurons undergoing CRMP2 knockdown display a decrease in voltage-dependent Ca^{2+} currents. It has been suggested, that intracellular CRMP2 action involves proper N-type VDCC trafficking and transmitter release (Brittain et al.,

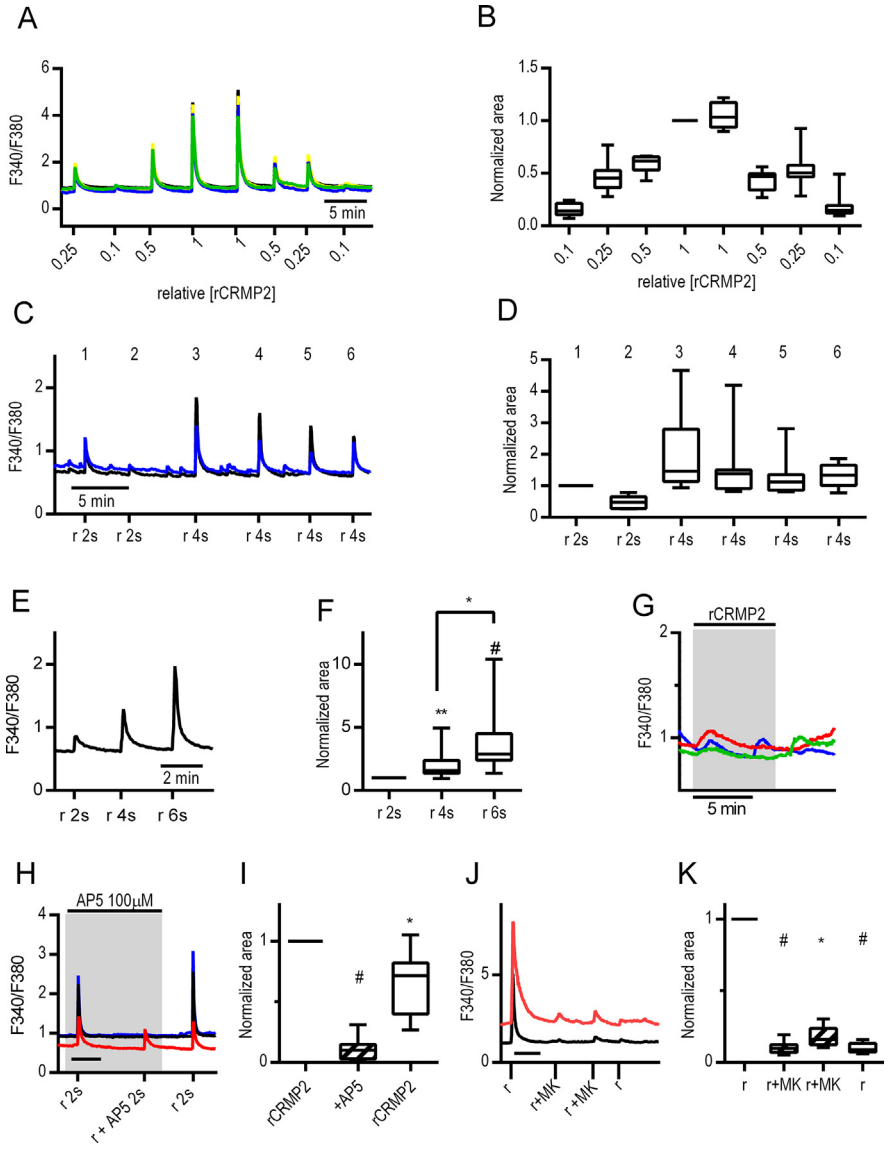

Fig. 10. Recombinant CRMP2 (rCRMP2) increases calcium through NMDA receptors. (A) Effect of different relative concentrations of rCRMP2 on the evoked $[Ca^{2+}]_i$ increase. The concentration range used was 30–300 nM. Representative traces of the response to the focal application of different rCRMP2 concentrations on hippocampal neurons. Pulses were applied for 2 s. (B) Normalized quantification of the areas under the curve shown in (A) (C) Focal application of consecutive rCMP2 pulses. (D) Box and whiskers of the results shown in (C). (E) Application of different time pulses. (F) Quantification of the areas under the curve shown in C ($^{**}=p = 0.0096$; $^{\#}=p < 0.0001$, and 4 s vs 6 s $p = 0.05$, Kruskal–Wallis $H = 28.6$, df = 2; $n = 15$; two experiments). (G) Example traces of the response to the continuous application of ~150 nM rCRMP2. (H) Example traces of the effect of AP5 on rCRMP2 evoked calcium increase. Scale is 2 min. (I) Quantification of the areas under the curve of rCRMP2 evoked calcium increase and in the presence of AP5 respectively (; (median block = 89% IQR 85–97, $p < 0.0001$; $n = 16$ and after removing AP-5 a recovery of 72%, IQR = 40–82 was obtained, $^{*}=0.01$, $n = 16$). (J) Example traces showing the effect of MK-801 50 μM on rCRMP2 evoked $[Ca^{2+}]$. Scale is 2 min. (K) Quantification of the areas under the curve shown in (H) (median block 90%, IQR = 87–93, $^{\#}=p < 0.0001$, for the first pulse; 84%, IQR 76–87, $^{*}p = 0.0442$ for the second pulse and after MK-801 was removed no recovery was observed: median block 91%, IQR = 87–93, $p < 0.0001$, Kruskal–Wallis $H = 28.4$, df = 3; $n = 10$). Distinct color traces correspond to different neuron responses under the condition stated in each panel. (For interpretation of the references to colour in this figure legend, the reader is referred to the web version of this article.)

2009; Chi et al., 2009). Moreover, it was demonstrated that the tat-CBD3 peptide interferes with N-type VDCC trafficking and consequently, inhibits transmitter release (Brittain et al., 2011b). Concerning the NMDAr, Al-Hallaq and coworkers (2007) showed that CRMP2 associates intracellularly with the NR2B subunit and the tat-CBD3 peptide interferes with this interaction, attenuating its response to NMDA (Brustovetsky et al., 2014). Therefore, as far as we know all the reported CRMP2 actions involve intracellular protein interactions.

The present study represents the first report showing that CRMP2 can act extracellularly probably by interacting with NMDAr and such interaction results in an increase in $[Ca^{2+}]_i$. Fig. 12 shows a schematic representation of how CRMP2-CM may be acting at the extracellular level. CRMP2-CM could bind directly to the NMDAr allowing NMDAr activation and hence increase in Ca^{2+} influx. This is supported by the fact that three different NMDAr antagonists are capable of strongly (~85%) blocking the CM-evoked $[Ca^{2+}]_i$ increase. CM could depolarize the cell (Fig. 5I), hence will open N-Type VDCC, which in turn activates glutamate and glycine release. Previously, it has been shown that block of N-type VDCC with ω-conotoxin GVIA, reduced glutamate and glycine release (Brittain et al., 2011b). In consequence, the released glycine and glutamate would be available to increase the activation of NMDAr. The released glutamate will also result in the activation of AMPA and Kainite receptors. This would explain why CM-evoked $[Ca^{2+}]_i$ increase was partially blocked by ω-conotoxin GVIA (~30%) and CNQX (~20). In summary, CRMP2 induces the $[Ca^{2+}]_i$ increase through activation of NMDAr, which it is potentiated by the glutamate/glycine released through the CM-mediated activation of N-type VDCC.

It was also investigated if some other molecules in the CM could be contributing to the CM-evoked $[Ca^{2+}]_i$ increase. For instance, we used a generic ErbB receptor (ErbBr) inhibitor (PD158780) to block neuregulin action, a protein that is present in the CM (Villegas et al., 2000). This inhibitor, instead of blocking the CM-evoked $[Ca^{2+}]_i$ increase, it potentiated the CM-evoked response, in agreement with NRG-1 blockage of LTP by suppressing phosphorylation

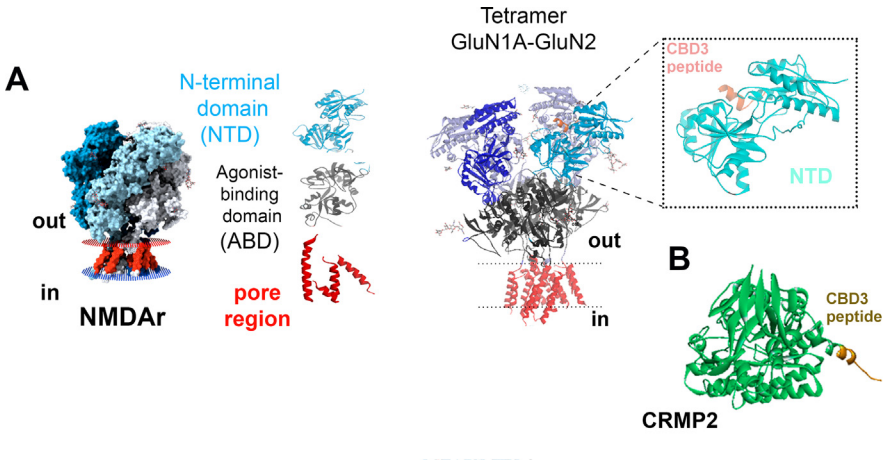

Fig. 11. *In silico* study showing that CRMP2 could bind to NMDAr. (A) Molecular architecture of NMDArs (right). Domain organization of an individual subunit. X-ray crystal structure of a full NMDAr GluN1A-GluN2B tetramer (PDB entry 4pe5). The NTDs are depicted in blue (GluN2B) and gray (GluN1A), the ABDs in black, the pore region in red (center). Docking showing 4pe5-CBD3 peptide complex (left). (B) Molecular architecture of a CRMP2 monomer (PDB entry 5uqc). The peptide CBD3 are depicted in orange. All structures were prepared with Discovery Studio 3.5 (Accelrys, USA, 2013). (For interpretation of the references to color in this figure legend, the reader is referred to the web version of this article.)

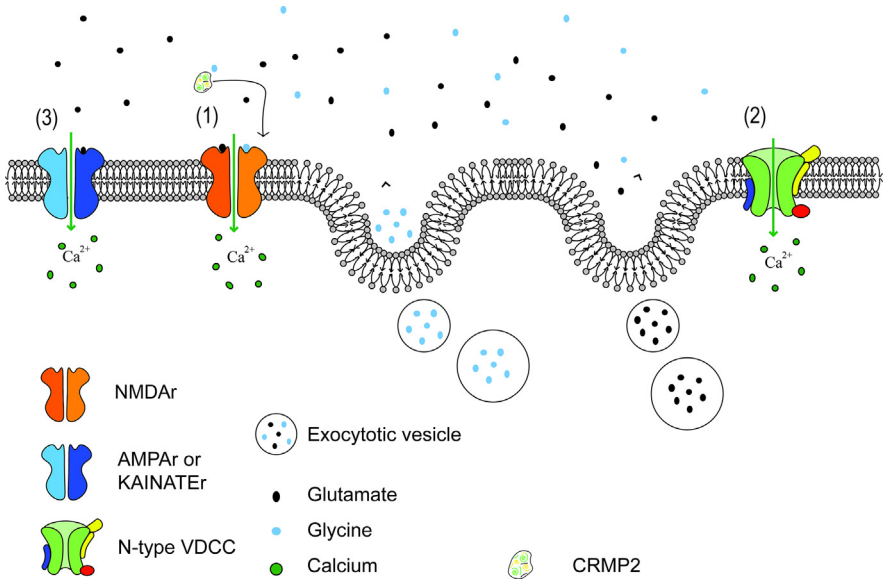

Fig. 12. Model depicting possible mode of action of extracellular CRMP2-CM on NMDAr and N-type VDCC. (1) CRMP2-CM binds directly to the NMDAr allowing Ca^{2+} influx into the cell, possibility supported by the fact that 3 different antagonists are capable of blocking the CM-evoked calcium increase. (2) CM could induce cell depolarization inducing opening of N-type VDCC, consequently inducing Ca^{2+} influx and promoting glutamate exocytosis. The released glutamate binds to the NMDAr to promote its opening and concurrent Ca^{2+} increase. At the same time, glycine would be released upon depolarization due to the calcium influx and both (glutamate and glycine) will open the NMDAr. This route is supported by the following results: ω-conotoxin GVIA is capable of blocking the CM-evoked calcium increase by 35% and (3) CNQX decreases 20% the response of the AMPA and kainite receptors that would also be opened by the glutamate release. Approximately, 85% of the response blocked by AP-5 should be in part due to the direct effect of CRMP2 on the NMDAr and the rest to the glutamate action on the receptors.

of NMDAr (Ma et al., 2003). Two other ErbBr inhibitors, AG825 (ErbB2 inhibitor) together with PD168393 (EGFr and erbB2, erbB4 inhibitor) did not block the CM-evoked response, if anything they slowed the decay of the response following CM removal. Neither the blocker of a related ErbB receptor, the EGF receptor inhibitor (AG30) nor the k252a (a generic TRK receptor inhibitor) affected the CM-evoked response. A blocker of store-operated Ca^{2+} entry and IP3 receptor (2-APB) also slowed the decay of the response following CM removal. However, the difference in decay between the CM- and the rCRMP2-evoked responses suggests that there could be other molecules in the CM that are modulating the CRMP2 effect, probably by slowing down desensitization of NMDAr.

The results suggest that CRMP2 released from injured nerves may activate NMDAr of nearby neurons and hence contribute to calcium dysregulation and further neuronal death. Excitotoxicity induced by excessive stimulation of the NMDAr has been related to numerous neurodegenerative diseases. In a model of optic neuritis induced by myelin oligodendrocyte glycoprotein (MOG), it was found that blocking NMDAr with MK-801 protected Retinal Ganglion cells (RGC) and oligodendrocytes from MOG-induced neurodegeneration (Sühs et al., 2014). Other neurodegenerative disorders where CRMP2 has been related may have dysregulation in calcium metabolism as a common link (Khanna et al., 2012). Additionally, a review of the proteins that could be involved in the onset of Alzheimer disease (AD), other than the amyloid β-protein precursor and tau, suggest that CRMP2 could be a good candidate to be investigated in the search of therapeutic targeting for AD (Hensley and Kursula, 2016).

CONCLUSION

We have demonstrated that CRMP2 is responsible for increasing intracellular Ca^{2+} in neurons by acting extracellularly mainly via NMDAr with a minor contribution from N-type VDCC. Release of CRMP2 could be a new way of signaling under specific physiological situations. As CRMP2 evokes calcium increase through the NMDAr and hence, modulates intracellular calcium signaling, therefore, the focal presence of extracellular CRMP2 could be another mechanism for regulating neurite outgrowth. This could happen in a similar way as the reported effect of

glutamate on NMDAr and neurite regulation (Pearce et al., 1987). Moreover, continuous presence of CRMP2 in the extracellular medium has a negative effect on calcium metabolism leading to pathological conditions that has not been considered until now. This is very important, since it would justify using CRMP2 as a therapeutic target to control neurotoxic or neurodegenerative processes.

AUTHOR CONTRIBUTIONS

CC and JCM designed the experiments and wrote the manuscript. CC performed imaging experiments, analyzed data and prepared the figures. LC, JLE performed Glu- Gly HPLC quantifications and YR prepared and performed the assay for glutamate and glycine measurements. ML designed and performed the experiments for live antibody labeling analysis and participated in manuscript preparation. HR made the confocal analysis. JCM and LG designed IP experiments. LG, performed some calcium imaging experiments, performed IP experiments. DH, initial calcium imaging experiments. LM, Western Blots and calcium imaging experiments, preparation of CM for imaging experiments. JC, Western Blots, IP, live imaging and figure preparations. MH and ML, purification and preparation of MC, WB. DB, ML and RV purification and preparation of samples for microsequencing and analysis of results. All authors reviewed and edited the manuscript.

This work is dedicated to the memory of Raimundo Villegas.

COMPETING FINANCIAL INTERESTS

The authors declare no competing financial interests.

ACKNOWLEDGMENTS

We thank Vet. Emilia Negron, German Guevara and all the Bioterio personnel for providing the animals. Jorge Nuñez for the CMs preparation, Elias Majul and Daniel Rojas for technical assistance. We also thank Dr. Dirk Hermann (University Hospital-Essen, Germany) for providing some of the reagents. This research was supported by IDEA-Venezuela and grant from FONACIT-Venezuela S1-200000641.

REFERENCES

Al-Hallaq RA, Conrads TP, Veenstra TD, Wenthold RJ (2007) NMDA di-heteromeric receptor populations and associated proteins in rat hippocampus. J Neurosci 27:8334–8343.

Berridge MJ (1998) Neuronal calcium signaling. Neuron 21:13–26.

Brewer GJ (1995) Serum-free B27/neurobasal medium supports differentiated growth of neurons from the striatum, substantia nigra, septum, cerebral cortex, cerebellum, and dentate gyrus. J Neurosci Res 42:674–683.

Brittain JM, Piekarz AD, Wang Y, Kondo T, Cummins TR, Khanna R (2009) An atypical role for collapsin response mediator protein 2 (CRMP-2) in neurotransmitter release via interaction with presynaptic voltage-gated calcium channels. J Biol Chem 284:31375–31390.

Brittain JM et al (2011a) Suppression of inflammatory and neuropathic pain by uncoupling CRMP-2 from the presynaptic Ca^{2+} channel complex. Nat Med 17:822–829.

Brittain JM, Chen L, Wilson SM, Brustovetsky T, Gao X, Ashpole NM, Molosh AI, You H, Hudmon A, Shekhar A, White FA, Zamponi GW, Brustovetsky N, Chen J, Khanna R (2011b) Neuroprotection against traumatic brain injury by a peptide derived from the collapsin response mediator protein 2 (CRMP2). J Biol Chem 286:37778–37792.

Brittain JM, Pan R, You H, Brustovetsky T, Brustovetsky N, Zamponi GW, Lee W-H, Khanna R (2012) Disruption of NMDAR-CRMP-2 signaling protects against focal cerebral ischemic damage in the rat middle cerebral artery occlusion model. Channels Austin Tex 6:52–59.

Brown KJ, Seol H, Pillai DK, Sankoorikal B-J, Formolo CA, Mac J, Edwards NJ, Rose MC, Hathout Y (2013) The human secretome atlas initiative: implications in health and disease conditions. Biochim Biophys Acta 1834:2454–2461.

Brustovetsky T, Pellman JJ, Yang X-F, Khanna R, Brustovetsky N (2014) Collapsin response mediator protein 2 (CRMP2) interacts with N-methyl-D-aspartate (NMDA) receptor and Na+/Ca2+ exchanger and regulates their functional activity. J Biol Chem 289:7470–7482.

Castillo C, Carreño F, Villegas GM, Villegas R (2001) Ionic currents in PC12 cells differentiated into neuron-like cells by a cultured-sciatic nerve conditioned medium. Brain Res 911:181–192.

Castillo C, Malavé C, Martínez JC, Núñez J, Hernández D, Pasquali F, Villegas GM, Villegas R (2006) Neuregulin-1 isoform induces mitogenesis, KCa and Ca2+ currents in PC12 cells. A comparison with sciatic nerve conditioned medium. Brain Res 1110:64–75.

Castillo C, Norcini M, Baquero-Buitrago J, Levacic D, Medina R, Montoya-Gacharna JV, Blanck TJJ, Dubois M, Recio-Pinto E (2011) The N-methyl-D-aspartate-evoked cytoplasmic calcium increase in adult rat dorsal root ganglion neuronal somata was potentiated by substance P pretreatment in a protein kinase C-dependent manner. Neuroscience 177:308–320.

Castillo C, Norcini M, Martin Hernandez LA, Correa G, Blanck TJJ, Recio-Pinto E (2013) Satellite glia cells in dorsal root ganglia express functional NMDA receptors. Neuroscience 240:135–146.

Chi XX, Schmutzler BS, Brittain JM, Wang Y, Hingtgen CM, Nicol GD, Khanna R (2009) Regulation of N-type voltage-gated calcium channels (Cav2.2) and transmitter release by collapsin response mediator protein-2 (CRMP-2) in sensory neurons. J Cell Sci 122:4351–4362.

Chiasserini D, van Weering JRT, Piersma SR, Pham TV, Malekzadeh A, Teunissen CE, de Wit H, Jiménez CR (2014) Proteomic analysis of cerebrospinal fluid extracellular vesicles: a comprehensive dataset. J Proteomics 106:191–204.

Chiku T, Padovani D, Zhu W, Singh S, Vitvitsky V, Banerjee R (2009) H2S biogenesis by human cystathionine gamma-lyase leads to the novel sulfur metabolites lanthionine and homolanthionine and is responsive to the grade of hyperhomocysteinemia. J Biol Chem 284:11601–11612.

Cline HT, Debski EA, Constantine-Paton M (1987) N-methyl-D-aspartate receptor antagonist desegregates eye-specific stripes. Proc Natl Acad Sci U S A 84:4342–4345.

Corrales A, Xu F, Garavito-Aguilar Z, Blanck TJJ, Recio-Pinto E (2003) Isoflurane reduction of carbachol-evoked cytoplasmic calcium transients is dependent on caffeine-sensitive calcium stores. Anesthesiology 99:882–888.

Cortazar AR, Oguiza JA, Aransay AM, Lavín JL (2017) VerSeDa: vertebrate secretome database. Database J Biol Databases Curation.

Courtney MJ, Lambert JJ, Nicholls DG (1990) The interactions between plasma membrane depolarization and glutamate receptor activation in the regulation of cytoplasmic free calcium in cultured cerebellar granule cells. J Neurosci Off J Soc Neurosci 10:3873–3879.

Davies SN, Lodge D (1987) Evidence for involvement of N-methylaspartate receptors in "wind-up" of class 2 neurones in the dorsal horn of the rat. Brain Res 424:402–406.
Dickenson AH, Sullivan AF (1987) Evidence for a role of the NMDA receptor in the frequency dependent potentiation of deep rat dorsal horn nociceptive neurones following C fibre stimulation. Neuropharmacology 26:1235–1238.
Foster AC, Kemp JA (1989) HA-966 antagonizes N-methyl-D-aspartate receptors through a selective interaction with the glycine modulatory site. J Neurosci Off J Soc Neurosci 9:2191–2196.
François-Moutal L, Wang Y, Moutal A, Cottier KE, Melemedjian OK, Yang X, Wang Y, Ju W, Largent-Milnes TM, Khanna M, Vanderah TW, Khanna R (2015) A membrane-delimited N-myristoylated CRMP2 peptide aptamer inhibits CaV2.2 trafficking and reverses inflammatory and postoperative pain behaviors. Pain 156:1247–1264.
Goshima Y, Nakamura F, Strittmatter P, Strittmatter SM (1995) Collapsin-induced growth cone collapse mediated by an intracellular protein related to UNC-33. Nature 376:509–514.
Grienberger C, Konnerth A (2012) Imaging calcium in neurons. Neuron 73:862–885.
Hensley K, Kursula P (2016) Collapsin Response Mediator Protein-2 (CRMP2) is a Plausible Etiological Factor and Potential Therapeutic Target in Alzheimer's Disease: Comparison and Contrast with Microtubule-Associated Protein Tau. J Alzheimers Dis JAD 53:1–14.
Hou ST, Jiang SX, Desbois A, Huang D, Kelly J, Tessier L, Karchewski L, Kappler J (2006) Calpain-cleaved collapsin response mediator protein-3 induces neuronal death after glutamate toxicity and cerebral ischemia. J Neurosci Off J Soc Neurosci 26:2241–2249.
Hou ST, Jiang SX, Aylsworth A, Ferguson G, Slinn J, Hu H, Leung T, Kappler J, Kaibuchi K (2009) CaMKII phosphorylates collapsin response mediator protein 2 and modulates axonal damage during glutamate excitotoxicity. J Neurochem 111:870–881.
Huettner JE, Bean BP (1988) Block of N-methyl-D-aspartate-activated current by the anticonvulsant MK-801: selective binding to open channels. Proc Natl Acad Sci U S A 85:1307–1311.
Inagaki N, Chihara K, Arimura N, Ménager C, Kawano Y, Matsuo N, Nishimura T, Amano M, Kaibuchi K (2001) CRMP-2 induces axons in cultured hippocampal neurons. Nat Neurosci 4:781–782.
Johnson JW, Ascher P (1987) Glycine potentiates the NMDA response in cultured mouse brain neurons. Nature 325:529–531.
Katano T, Mabuchi T, Okuda-Ashitaka E, Inagaki N, Kinumi T, Ito S (2006) Proteomic identification of a novel isoform of collapsin response mediator protein-2 in spinal nerves peripheral to dorsal root ganglia. Proteomics 6:6085–6094.
Khanna R, Wilson SM, Brittain JM, Weimer J, Sultana R, Butterfield A, Hensley K (2012) Opening Pandora's jar: a primer on the putative roles of CRMP2 in a panoply of neurodegenerative, sensory and motor neuron, and central disorders. Future Neurol 7:749–771.
Kleinschmidt A, Bear MF, Singer W (1987) Blockade of "NMDA" receptors disrupts experience-dependent plasticity of kitten striate cortex. Science 238:355–358.
Kroksveen AC, Guldbrandsen A, Vaudel M, Lereim RR, Barsnes H, Myhr K-M, Torkildsen Ø, Berven FS (2017) In-Depth Cerebrospinal Fluid Quantitative Proteome and Deglycoproteome Analysis: Presenting a Comprehensive Picture of Pathways and Processes Affected by Multiple Sclerosis. J Proteome Res 16:179–194.
Kuter K, Kratochwil M, Marx S-H, Hartwig S, Lehr S, Sugawa MD, Dencher NA (2016) Native DIGE proteomic analysis of mitochondria from substantia nigra and striatum during neuronal degeneration and its compensation in an animal model of early Parkinson's disease. Arch Physiol Biochem 122:238–256.
Lerma J, Zukin RS, Bennett MV (1990) Glycine decreases desensitization of N-methyl-D-aspartate (NMDA) receptors expressed in Xenopus oocytes and is required for NMDA responses. Proc Natl Acad Sci U S A 87:2354–2358.
Lester RA, Jahr CE (1992) NMDA channel behavior depends on agonist affinity. J Neurosci Off J Soc Neurosci 12:635–643.
Levy E (2017) Exosomes in the Diseased Brain: First Insights from In vivo Studies. Front Neurosci 11:142.
López E, Hernandez J, Arce C, Cañadas S, Oset-Gasque MJ, González MP (2010) Involvement of NMDA receptor in the modulation of excitatory and inhibitory amino acid neurotransmitters release in cortical neurons. Neurochem Res 35:1478–1486.
Ma L, Huang YZ, Pitcher GM, Valtschanoff JG, Ma YH, Feng LY, Lu B, Xiong WC, Salter MW, Weinberg RJ, Mei L (2003) Ligand-dependent recruitment of the ErbB4 signaling complex into neuronal lipid rafts. J Neurosci Off J Soc Neurosci 23:3164–3175.
Malavé C, Villegas GM, Hernández M, Martínez JC, Castillo C, Suárez de Mata Z, Villegas R (2003) Role of glypican-1 in the trophic activity on PC12 cells induced by cultured sciatic nerve conditioned medium: identification of a glypican-1-neuregulin complex. Brain Res 983:74–83.
Menon KN, Steer DL, Short M, Petratos S, Smith I, Bernard CCA (2011) A novel unbiased proteomic approach to detect the reactivity of cerebrospinal fluid in neurological diseases. Mol Cell Proteomics MCP 10(M110):000042.
Moutal A, François-Moutal L, Brittain JM, Khanna M, Khanna R (2015) Differential neuroprotective potential of CRMP2 peptide aptamers conjugated to cationic, hydrophobic, and amphipathic cell penetrating peptides. Front Cell Neurosci 8:471.
Moutal A, Eyde N, Telemi E, Park KD, Xie JY, Dodick DW, Porreca F, Khanna R (2016) Efficacy of (S)-Lacosamide in preclinical models of cephalic pain. Pain Rep:1.
Moutal A, Cai S, Luo S, Voisin R, Khanna R (2017a) CRMP2 is necessary for neurofibromatosis type 1 related pain. Channels Austin Tex.
Moutal A, Dustrude ET, Largent-Milnes TM, Vanderah TW, Khanna M, Khanna R (2017b) Blocking CRMP2 SUMOylation reverses neuropathic pain. Mol Psychiatry.
Moutal A, Li W, Wang Y, Ju W, Luo S, Cai S, François-Moutal L, Perez-Miller S, Hu J, Dustrude ET, Vanderah TW, Gokhale V, Khanna M, Khanna R (2017c) Homology-guided mutational analysis reveals the functional requirements for antinociceptive specificity of collapsin response mediator protein 2-derived peptides. Br J Pharmacol.
Moutal A, Wang Y, Yang X, Ji Y, Luo S, Dorame A, Bellampalli SS, Chew LA, Cai S, Dustrude ET, Keener JE, Marty MT, Vanderah TW, Khanna R (2017d) Dissecting the role of the CRMP2-neurofibromin complex on pain behaviors. Pain 158:2203–2221.
Moutal A, Yang X, Li W, Gilbraith KB, Luo S, Cai S, François-Moutal L, Chew LA, Yeon SK, Bellampalli SS, Qu C, Xie JY, Ibrahim MM, Khanna M, Park KD, Porreca F, Khanna R (2017e) CRISPR/Cas9 editing of Nf1 gene identifies CRMP2 as a therapeutic target in neurofibromatosis type 1-related pain that is reversed by (S)-Lacosamide. Pain 158:2301–2319.
Nunez J (2008) Primary Culture of Hippocampal Neurons from P0 Newborn Rats. J Vis Exp Available at: http://www.jove.com/index/Details.stp?ID=895 [Accessed June 12, 2017].
Paoletti P (2011) Molecular basis of NMDA receptor functional diversity. Eur J Neurosci 33:1351–1365.
Pearce IA, Cambray-Deakin MA, Burgoyne RD (1987) Glutamate acting on NMDA receptors stimulates neurite outgrowth from cerebellar granule cells. FEBS Lett 223:143–147.
Petratos S, Ozturk E, Azari MF, Kenny R, Lee JY, Magee KA, Harvey AR, McDonald C, Taghian K, Moussa L, Mun Aui P, Siatskas C, Litwak S, Fehlings MG, Strittmatter SM, Bernard CCA (2012) Limiting multiple sclerosis related axonopathy by blocking Nogo receptor and CRMP-2 phosphorylation. Brain J Neurol 135:1794–1818.
Prudovsky I, Tarantini F, Landriscina M, Neivandt D, Soldi R, Kirov A, Small D, Kathir KM, Rajalingam D, Kumar TKS (2008) Secretion without Golgi. J Cell Biochem 103:1327–1343.

Rogemond V, Auger C, Giraudon P, Becchi M, Auvergnon N, Belin M-F, Honnorat J, Moradi-Améli M (2008) Processing and nuclear localization of CRMP2 during brain development induce neurite outgrowth inhibition. J Biol Chem 283:14751–14761.

Schmidt EF, Strittmatter SM (2007) The CRMP family of proteins and their role in Sema3A signaling. Adv Exp Med Biol 600:1–11.

Schneider A, Simons M (2013) Exosomes: vesicular carriers for intercellular communication in neurodegenerative disorders. Cell Tissue Res 352:33–47.

Scholz KP, Miller RJ (1995) Developmental changes in presynaptic calcium channels coupled to glutamate release in cultured rat hippocampal neurons. J Neurosci Off J Soc Neurosci 15:4612–4617.

Schutzer SE, Liu T, Natelson BH, Angel TE, Schepmoes AA, Purvine SO, Hixson KK, Lipton MS, Camp DG, Coyle PK, Smith RD, Bergquist J (2010) Establishing the proteome of normal human cerebrospinal fluid. PLoS ONE 5:e10980.

Sühs K-W, Fairless R, Williams SK, Heine K, Cavalié A, Diem R (2014) N-methyl-D-aspartate receptor blockade is neuroprotective in experimental autoimmune optic neuritis. J Neuropathol Exp Neurol 73:507–518.

Sutachan J-J, Montoya GJV, Xu F, Chen D, Blanck TJJ, Recio-Pinto E (2006) Pluronic F-127 affects the regulation of cytoplasmic Ca2 + in neuronal cells. Brain Res 1068:131–137.

Suzuki Y, Nakagomi S, Namikawa K, Kiryu-Seo S, Inagaki N, Kaibuchi K, Aizawa H, Kikuchi K, Kiyama H (2003) Collapsin response mediator protein-2 accelerates axon regeneration of nerve-injured motor neurons of rat. J Neurochem 86:1042–1050.

Villegas GM, Haustein AT, Villegas R (1995) Neuronal differentiation of PC12 and chick embryo ganglion cells induced by a sciatic nerve conditioned medium: characterization of the neurotrophic activity. Brain Res 685:77–90.

Villegas R, Villegas GM, Longart M, Hernández M, Maqueira B, Buonanno A, García R, Castillo C (2000) Neuregulin found in cultured-sciatic nerve conditioned medium causes neuronal differentiation of PC12 cells. Brain Res 852:305–318.

Villegas R, Villegas GM, Núñez J, Hernández M, Castillo C (2005) Neuron-like differentiation of PC12 cells treated with media conditioned by either sciatic nerves, optic nerves, or Schwann cells. Cell Mol Neurobiol 25:451–461.

Wang Y, Brittain JM, Wilson SM, Khanna R (2010) Emerging roles of collapsin response mediator proteins (CRMPs) as regulators of voltage-gated calcium channels and synaptic transmission. Commun Integr Biol 3:172–175.

Wen Z, Guirland C, Ming G-L, Zheng JQ (2004) A CaMKII/calcineurin switch controls the direction of Ca(2 +)-dependent growth cone guidance. Neuron 43:835–846.

Wu C-C, Chen H-C, Chen S-J, Liu H-P, Hsieh Y-Y, Yu C-J, Tang R, Hsieh L-L, Yu J-S, Chang Y-S (2008) Identification of collapsin response mediator protein-2 as a potential marker of colorectal carcinoma by comparative analysis of cancer cell secretomes. Proteomics 8:316–332.

Xie JY, Chew LA, Yang X, Wang Y, Qu C, Wang Y, Federici LM, Fitz SD, Ripsch MS, Due MR, Moutal A, Khanna M, White FA, Vanderah TW, Johnson PL, Porreca F, Khanna R (2016) Sustained relief of ongoing experimental neuropathic pain by a CRMP2 peptide aptamer with low abuse potential. Pain 157:2124–2140.

Yoshida H, Watanabe A, Ihara Y (1998) Collapsin response mediator protein-2 is associated with neurofibrillary tangles in Alzheimer's disease. J Biol Chem 273:9761–9768.

Yoshimura T, Kawano Y, Arimura N, Kawabata S, Kikuchi A, Kaibuchi K (2005) GSK-3beta regulates phosphorylation of CRMP-2 and neuronal polarity. Cell 120:137–149.

Zhang Y, Guo Z, Zou L, Yang Y, Zhang L, Ji N, Shao C, Sun W, Wang Y (2015a) A comprehensive map and functional annotation of the normal human cerebrospinal fluid proteome. J Proteomics 119:90–99.

Zhang Y, Guo Z, Zou L, Yang Y, Zhang L, Ji N, Shao C, Wang Y, Sun W (2015b) Data for a comprehensive map and functional annotation of the human cerebrospinal fluid proteome. Data Brief 3:103–107.

(Received 11 July 2017, Accepted 2 February 2018)